Organic Geochemistry 40 (2009) 87–110

Contents lists available at ScienceDirect

Organic Geochemistry

journal homepage: www.elsevier.com/locate/orggeochem

Origin of petroleum in the Neoproterozoic–Cambrian South Oman Salt Basin

E. Grosjean [a,*], G.D. Love [a,1], C. Stalvies [b], D.A. Fike [a], R.E. Summons [a]

[a] Department of Earth, Atmospheric and Planetary Sciences, Massachusetts Institute of Technology, 77 Massachusetts Avenue, Cambridge, MA 02139, USA
[b] Newcastle Research Group, University of Newcastle, Newcastle upon Tyne NE1 7 RU, UK

ARTICLE INFO

Article history:
Received 3 December 2007
Received in revised form 25 August 2008
Accepted 5 September 2008
Available online 10 October 2008

ABSTRACT

The South Oman Salt Basin (SOSB) is host to the world's oldest known commercial deposits. Most of the South Oman oils have been proven to be associated with the source rocks of the Neoproterozoic to Cambrian Huqf Supergroup, but the assignment of oils to specific Huqf intervals or facies has been hampered by the geochemical similarity of the organic matter across the entire Huqf sequence, possibly as a consequence of limited change in the local palaeoenvironment and biota over the time of its deposition. This study was conducted to establish improved correlations between organic-rich rock units and reservoir fluids in the SOSB through detailed molecular and isotopic analysis of the Huqf Supergroup, with special emphasis directed towards understanding the Ara carbonate stringer play.

Unusual biomarkers, tentatively identified as A-norsteranes, show distinctive patterns among carbonate stringer oils and rocks different from those observed in Nafun sediments and Ara rocks from the Athel basin. These putative A-norsteranes form the basis for new oil-source correlations in the SOSB and provide for the first time geochemical evidence of a self-charging mechanism for the carbonate stringer play. The paucity of markers specific to the Nafun Group (Shuram, Buah and Masirah Bay formations) confounds attempts to quantify their respective contributions to Huqf oil accumulations. Nafun inputs can only be determined on the basis of subtle differences between Nafun and Ara biomarker ratios. The most useful geochemical characteristics delineating Nafun Group organic matter from Ara Group intra-salt source rocks included: low relative abundance of mid-chain monomethyl alkanes (X-compounds); low relative abundance of gammacerane, 28,30-dinorhopane, 25,28,30-trinorhopane and 2-methylhopanes; low $C_{22}T/C_{21}T$ and high $C_{23}T/C_{24}T$ cheilanthanes ratio values. Based on these parameters, molecular evidence for major contributions of liquid hydrocarbons from Nafun Group sediments (Shuram, Buah and Masirah Bay formations) is lacking. Our results suggest that the majority of SOSB hydrocarbon accumulations originate from within the Ara group, either from the carbonate stringers or from the package of sediments that comprises the Thuleilat, Athel Silicilyte and U shale formations. Subtle aspects of the composition of some carbonate stringer and post-salt Huqf oils could suggest some degree of sourcing from the Nafun rocks but stronger evidence is needed to confirm this.

1. Introduction

The South Oman Salt Basin (SOSB) is an unusual petroleum-producing domain as it is host to the world's oldest known commercial oil deposits. Two major oil types, the 'Huqf' and the 'Q' oils, were recognized over 20 years ago and are clearly distinguished on the basis of carbon isotopic composition and sterane carbon number distributions (Grantham, 1986; Grantham et al., 1987). The Huqf oils have abnormally low carbon isotope ratio values [typically −36‰ VPDB (Vienna Pee Dee Belemnite)] and a strong predominance of C_{29} steranes, in contrast to the Q oils characterized by carbon isotope values near −30‰ and C_{27}-dominated steranes. Both oil types show conspicuous mid-chain monomethyl alkanes, trivially named "X compounds", considered characteristic of Precambrian-Cambrian source rocks (Fowler and Douglas, 1987; Summons et al., 1988a,b; Bazhenova and Arefiev, 1997). As the organic matter (OM) within the Huqf source rocks displays similar characteristics to the Huqf oils, a straightforward correlation has been established between these oils and the Huqf Supergroup (Grantham, 1986; Grantham et al., 1987; Terken et al., 2001). On the other hand, the origin of the Q oils, clustered to the north of the SOSB and in the basins to the north, is a matter of speculation as the source rock remains unproven. A Precambrian source for the latter was proposed on the basis of the mid-chain monomethyl alkane presence and of their spatial and stratigraphic distributions (Grantham et al., 1987).

Studies to date have established the uniqueness of Oman's old Huqf petroleum systems. However, they have not provided suffi-

* Corresponding author. Present address: Geoscience Australia, GPO Box 378, Canberra, ACT 2601, Australia. Tel.: +61 2 6249 9017; fax: +61 2 6249 9961.
E-mail addresses: Emmanuelle.Grosjean@ga.gov.au, egrosjea@bigpond.net.au (E. Grosjean).
[1] Present address: University of California Riverside, 900 University Avenue, Riverside 92521, USA.

0146-6380/$ - see front matter Crown copyright © 2008 Published by Elsevier Ltd. All rights reserved.
doi:10.1016/j.orggeochem.2008.09.011

cient resolution to unequivocally unravel specific source to charge relationships needed to determine which, if any, carbonate reservoirs in the Huqf Precambrian–Cambrian Ara (Reinhardt et al., 1998; Al-Siyabi, 2005) are self-charged and whether and where older high quality, pre-Ara Precambrian source rocks of the Nafun group have contributed significantly to the charge. These are key questions which have a direct impact on the exploration of inter- and pre-Ara plays in the Oman salt basins. Improved correlations between organic-rich rock units and reservoir fluids in the SOSB would help establish the volumetric contributions of potential Ara and Nafun source rocks to the existing accumulations and provide a framework for basin modelling to reduce charge risk and enhance prospectivity.

The assignment of 'Huqf' oils to specific Huqf intervals or facies is hampered by an overall geochemical homogeneity of the OM across the whole Huqf sequence, possibly a consequence of limited biological diversity or limited environmental evolution over the time of deposition. Biomarker analysis of oils and rocks using gas chromatography–mass spectrometry (GC–MS) methods with selected ion monitoring (SIM) have largely failed to unambiguously and conclusively type oil to source rock intervals because of the remarkable uniformity of the sterane and triterpane distributions.

In order to improve our understanding of SOSB petroleum systems, a detailed organic geochemical study has been performed via thorough analysis of selected South Oman oils and Huqf rock samples. Conventional organic geochemical methods commonly applied to Phanerozoic petroleum systems are not necessarily optimal for such a study owing to the exceptionally old and unusual OM. Accordingly, we sought to identify geochemical indices tailored to these particular petroleum systems. Special emphasis was directed towards the understanding of the Huqf oils origin. While the Q oils geochemistry is briefly presented, the understanding of their charge is the focus of a companion paper where new findings about their potential source rocks are presented.

2. Geological setting

2.1. Stratigraphy and age constraints

The South Oman Salt Basin, located at the southeastern edge of the Arabian Peninsula, is developed on Pan-African basement and contains a Neoproterozoic–Early Cambrian sedimentary succession known as the Huqf Supergroup (Gorin et al., 1982; Loosveld et al., 1996). The Huqf Supergroup begins with a thick siliclastic unit (the Ghadir Manqil Fm. of the Abu Mahara Group), followed by two clastic-carbonate cycles (the Masirah Bay and Khufai, and the Shuram and Buah formations of the Nafun Group) and terminated by the chert-carbonate evaporite succession of the Ara Group (Grotzinger et al., 2002; Fig. 1). Recent studies provide a detailed sedimentological framework of the Masirah Bay (Allen and Leather, 2006), the Shuram (Le Guerroué et al., 2006a,b) and the Buah (Cozzi et al., 2004; Cozzi and Al-Siyabi, 2004) formations of the Nafun Group. Initial U/Pb geochronology, stable isotope chemostratigraphy, palaeontology and geological interpretation identified the Ghadir Manqil Fm. as a Sturtian age (ca. 723 Ma) glacio-marine diamictite (Brasier et al., 2000) and carbonates and shales within the A4 unit of the Ara Group as being deposited at the Neoproterozoic–Cambrian boundary at ca. 542 Ma (Amthor et al., 2003). New geochronological constraints (Bowring et al., 2007) indicate that the Huqf Supergroup was deposited on basement rocks of ca. 840 to 810 Ma age and that two glacial episodes are recorded at ca. 713 and < 645 Ma. Ash beds in the basal Ara Group (A0 carbonate) record an age of ca. 547 Ma for carbonate rocks that occur above strata marked by pronounced negative (−12‰) to positive excursion (+4‰) in carbon isotope composition of carbonates. Further overlying Ara strata contain ash beds within the basal A3C unit (ca. 543 Ma), the upper A3C unit (ca. 542 Ma) and the basal A4C unit (ca. 541 Ma), which approximates the Ediacaran–Cambrian boundary in Oman. The 16‰ carbon isotope excursion occurs within the

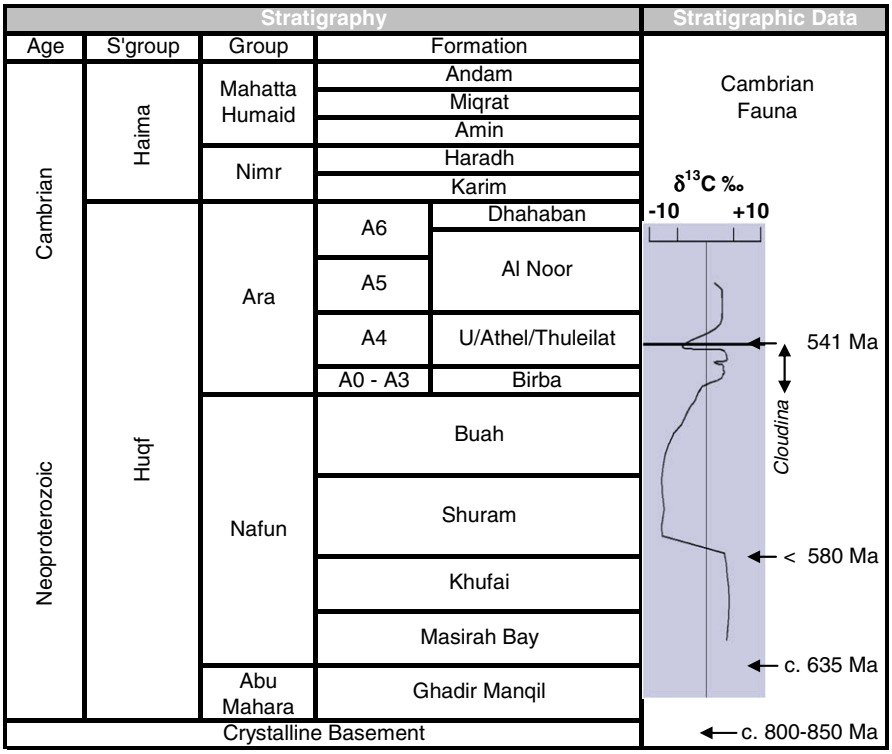

Fig. 1. Generalized stratigraphic column for Neoproterozoic and Early Cambrian strata of SOSB (modified from Amthor et al., 2005).

Shuram Fm., which has a firm maximum age of ca. 620 Ma, provided by the age of two detrital zircons in the basal part of the unit. The 'Shuram' excursion is a useful marker for global chemostratigraphic correlation (Halverson et al., 2002, 2005; Condon et al., 2005). Furthermore, patterns in sulfur isotopes (sulfate and pyrite) and carbon isotopes (carbonate and organic carbon) through the Nafun and Ara sequences indicate that these sediments were deposited during the period in which the Ediacaran ocean became fully oxygenated (Fike et al., 2006).

2.2. Palaeogeography

A detailed description of the palaeogeography and stratigraphy of the Ara group is provided by Amthor et al. (2005) and Schröder and Grotzinger (2007). Briefly, during deposition of the Ara group, the SOSB was subdivided into three separate palaeogeological domains: two platforms, the North and South Carbonate Platforms, separated by a deeper stratified basin (Athel Sub-basin; Fig. 2) with water depth potentially of several hundred meters in the deeper

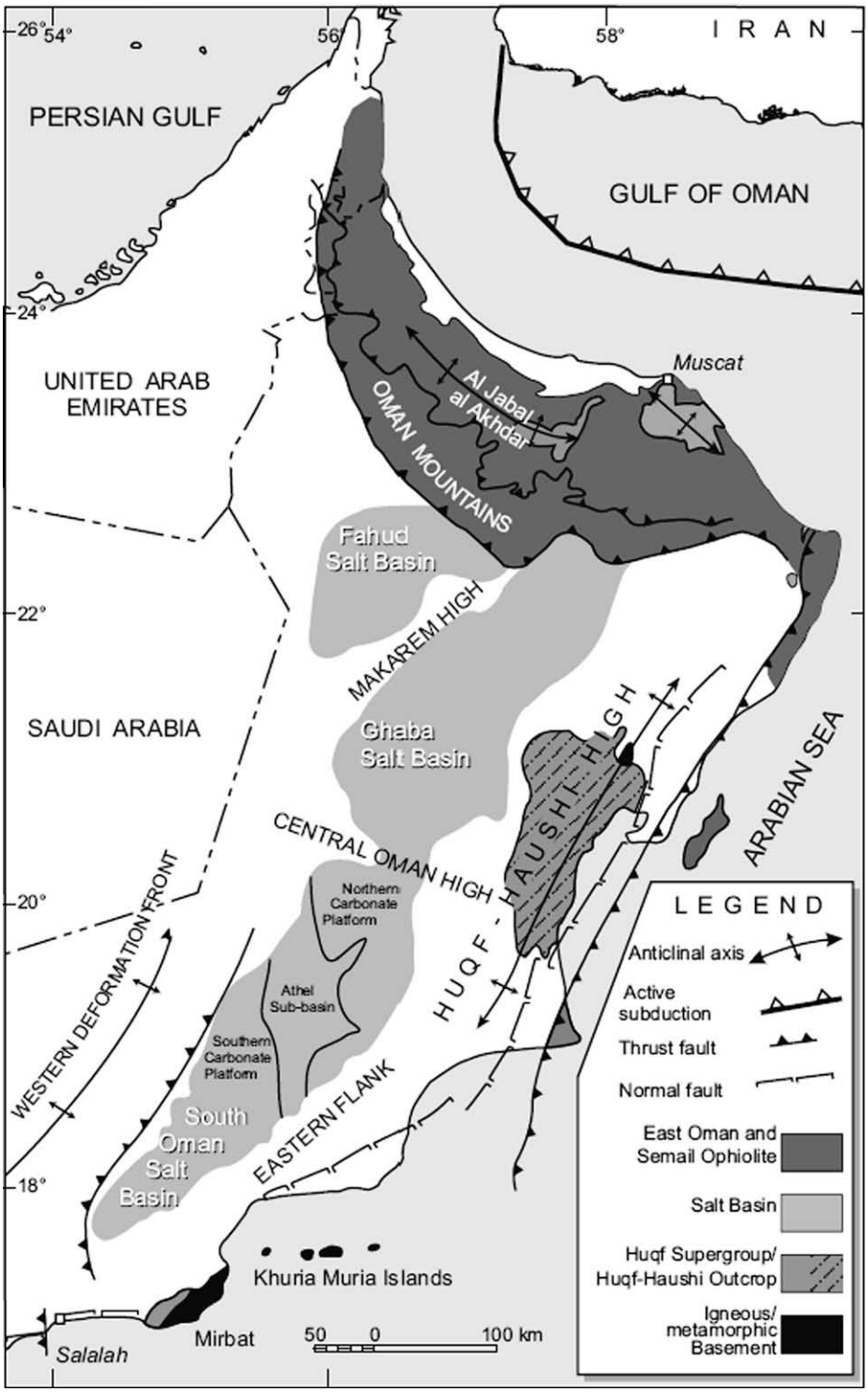

Fig. 2. Map of Oman showing main tectonic elements, positions of the salt basins and the structural setting of the South Oman Salt Basin (modified from Bowring et al., 2007).

depocentres (Mattes and Conway Morris, 1990; Amthor et al., 1998). The carbonate platforms consist of a cyclic succession of up to seven carbonate units, or 'stringers', each sandwiched within sulfate and halite evaporites (Mattes and Conway Morris, 1990). The tectono-eustatic evaporite–carbonate cycles are termed A0 to A6 from bottom to top. In the basin centre, the stratigraphic equivalent of the A4C unit consists of two organic-rich shale units, the U Shale Fm. and the Thuleilat Fm., bracketing the unique siliceous rocks of the Athel Silicilyte (aka Al Shomou Silicilyte; Amthor et al., 2005; Schröder and Grotzinger, 2007). Towards the eastern flank, stringers form an almost continuous carbonate platform due to salt withdrawal.

The rocks deposited within the Ara Group are commonly called intra-salt rocks, whereas rocks deposited before, including those of the Nafun Group, are referred to as pre-salt rocks. Hereafter, Ara source rocks deposited in the Athel Basin are referred to as Athel intra-salt rocks, as opposed to the Ara carbonate stringers.

2.3. Oil occurrences

Oils typed to the Huqf Supergroup source rocks, the so-called Huqf oils, are found within a number of structures in the Ara carbonate stringers, in the intra-salt Athel Silicilyte and in reservoirs of the Cambrian Haima and Permo-Carboniferous Haushi groups, particularly along the eastern flank of the SOSB (Al-Marjeby and Nash, 1986; Konert et al., 1991) and, as a result, are sub-divided according to their reservoirs in carbonate stringer oils, silicilyte oils and post-salt Huqf oils (also referred to as Eastern Flank oils), respectively. In contrast, Q oils occur mostly in Central Oman but can also be found in the northernmost part of the SOSB. Where encountered in the same well, Q oils occur in reservoirs that overlie those of the Huqf oils.

3. Methods

3.1. Bulk analysis

Rock-Eval parameters (Hydrogen Index HI, Oxygen Index OI and T_{max}) as well as total organic carbon (TOC) were determined using a Vinci Rock-Eval 6 apparatus according to established procedures (Espitalié et al., 1985). Samples were crushed and extracted with a mixture of dichloromethane (DCM) and MeOH (9:1, v/v) using a Dionex Accelerator Solvent Extractor ASE-200 operated under 1000 psi at 100 °C. Asphaltenes were precipitated out from the resulting organic extracts (bitumens) and from the oils using *n*-pentane. In asphaltene-free fractions (maltenes) derived from bitumens, elemental sulfur was removed with activated copper pellets. The maltenes were fractionated on a silica gel column, eluting successively with hexane, hexane/DCM (8:2, v/v) and DCM/MeOH (7:3, v/v) to give, respectively, alkanes, aromatic hydrocarbons and resins. Branched and cyclic alkanes were separated from *n*-alkanes by treatment with silicalite. Ca. 10 mg of alkanes, in a minimum volume of *n*-pentane were placed on a 3 cm bed of activated, crushed silicalite lightly packed into a Pasteur pipette. The non-adduct (SNA), containing branched and cyclic alkanes, was eluted using pentane (4 ml).

Bulk carbon isotope analysis was carried out using an elemental analyzer coupled to a Finnigan Delta Plus XP according to standard sealed tube combustion techniques (Sofer, 1980). Results ($\delta^{13}C$ values) are reported relative to the Vienna Peedee Belemnite (VPDB) standard. Hydropyrolysis of solvent-extracted samples were achieved according to the procedure described by Love et al. (1997).

3.2. Biomarker analysis

Gas-chromatography (GC) was carried out with a Hewlett–Packard 6890 chromatograph in splitless injection mode, equipped with a flame ionization detector (FID; 300 °C) and a Chrompack CPSil-5CB fused silica column (60 m × 0.32 mm i.d., 0.25 μm film thickness). He was used as carrier gas. Typical temperature programme was 60 °C (held 2 min) to 100 °C (10 °C/min) and to 315 °C (4 °C/min; held 30 min). Alkanes such as *n*-alkanes, pristane (Pr), phytane (Ph) and monomethyl alkanes (MMAs) were quantified using 3-methylheneicosane (ai-C_{22}) as internal standard.

Full scan gas chromatography–mass spectrometry (GC–MS) was carried out either with a Hewlett–Packard 5973 mass spectrometer connected to a Hewlett–Packard 6890 gas chromatograph equipped with a Chrompack CPSil-5CB fused silica column (60 m × 0.32 mm 0.25 μm film thickness), or with a Autospec Ultima mass spectrometer connected to a Hewlett–Packard 6890 gas chromatograph (J&W Scientific DB-1 column, 60 m × 0.25 mm i.d., 0.25 μm film thickness). Samples were injected in pulsed splitless mode. The oven was programmed from 60 °C (held 2 min) to 150 °C at 10 °C/min and at 3 °C/min to 315 °C (held 24 min). Mass spectra were produced at 70 eV and He was the carrier gas. For detailed GC–MS analysis of steranes and hopanes, samples were analyzed using the Autospec Ultima mass spectrometer operated in the metastable reaction monitoring (MRM) mode (same GC conditions as for full scan mode). Biomarkers such as steranes, hopanes and cheilanthanes, were detected using 26 individual precursor–product transitions sampled over a cycle of ca. 1.2 s and were quantified using d_4-ααα-ethylcholestane (D4) as internal standard without taking into account response factors. Biomarker ratios used in this study were obtained from MRM GC–MS analysis.

Principal components analysis (PCA) and hierarchical cluster analysis (HCA) were conducted using the Pirouette software (Infometrix Corporation).

4. Samples

4.1. Rocks

In total, 46 source rocks were provided (Table 1); 17 Nafun Group rocks, including 4 Masirah Bay Fm., 9 Shuram Fm. and 4 Buah Fm. samples, were analyzed. With respect to the Ara intra-salt section, 14 Athel intra-salt rocks, comprising 5 U Shale Fm., 5 Athel Silicylite, 4 Thuleilat Fm. samples and 15 carbonate stringers (1 × A1C, 2 × A2C, 5 × A3C, 5 × A4C, 2 × A5C) are reported in detail. Most of the samples were composites of cuttings taken over several 10 s of meter intervals in order to homogenize and, thereby, more completely characterize the geochemistry of the source rock formation. The exceptions were carbonate stringer samples and Buah Fm. sample OMR020 where only core material was available.

4.2. Oils

In total, 54 South Oman oils (6 Q oils and 48 Huqf oils) were examined. Huqf oils included 7 silicilyte oils, 15 post-salt Huqf oils and 26 carbonate stringer oils from A1C to A6C stratigraphic unit. Table 2 summarizes their bulk properties.

5. Source rock evaluation: overview

Bulk geochemical parameters are given in Table 1. High TOC rocks with petroleum source potential have been recognized in the intra-salt and pre-salt sections of the Huqf Supergroup for some time (Mattes and Conway Morris, 1990). In the Athel basin,

Table 1
Rock-Eval data and bulk carbon isotopic composition of alkane and aromatic hydrocarbon fractions of rocks (TOC, total organic carbon; HI, Hydrogen Index; OI, Oxygen index).

Formation	MIT ID	Well code	Well HID	Depth (m)	TOC (%wt)	HI	OI	T_{max} (°C)	$^{13}\delta$Sats	$^{13}\delta$Aros
A1C	OMR039	Ds	105417284148270	2997	1.22	339	47	429	−35.6	−35.6
A2C	OMR034	Bn	105518042847200	4204	1.9	451	46	435	−35.3	−35.1
A2C	OMR042	Sb	105518121015410	2399	1.19	352	42	437	−36.0	−36.1
A3C	OMR028	Bi	105518051934160	2927	0.53	314	106	428	NA	NA
A3C	OMR035	Bn	105518042847200	3790	0.19	276	329	440	−33.2	−34.7
A3C	OMR036	Bn	105518042847200	3789	0.4	321	124	435	NA	NA
A3C	OMR037	Bn	105518042847200	3787	0.72	358	121	423	−34.1	−34.7
A3C	OMR038	Bn	105518042847200	3785	0.13	325	505	440	NA	−34.7
A4C	OMR029	Br	105518061900350	2930	0.95	274	69	423	−34.5	−34.7
A4C	OMR030	Br	105518061900350	2928	0.57	338	99	425	−34.0	−34.4
A4C	OMR031	Br	105518061900350	2928	1.06	253	87	424	−34.4	−34.6
A4C	OMR032	Br	105518061900350	2920	0.56	303	98	429	NA	NA
A4C	OMR033	Bb	105518052021340	3009	1.92	482	33	434	−34.3	−34.4
A5C	OMR040	Om	105518022220500	2853	1.05	332	93	419	NA	NA
A5C	OMR041	Om	105518022220500	2851	0.44	338	168	419	−34.8	−34.9
Buah	OMR002	Am	105518431952210	2345–2375	1.6	278	33	426	NA	−38.4
Buah	OMR017	Sa	105618284827160	1569–1602	2.3	339	20	433	−38.7	−39.5
Buah	OMR020	Ta	105518505500411	4411	3.1	411	4	443	NA	−37.4
Buah	OMR149	At	105518471651420	2016–2019	11.0	NA	NA	NA	−37.4	−37.7
Masirah Bay	OMR016	Ru	105618074334180	3125–3143	1.7	419	58	431	−33.5	−34.1
Masirah Bay	OMR027	Za	105619334013330	2280–2295	3.8	338	45	425	−32.0	−31.2
Masirah bay	OMR153	Ss	105720133211290	4230–4385	0.4	NA	NA	NA	NA	NA
Masirah Bay	OMR157	Th	105518260443550	2895–2910	4.9	NA	NA	NA	NA	NA
Shuram	OMR010	Mb	105518381457000	2628–2724	2.5	397	11	437	−35.0	−34.5
Shuram	OMR026	Za	105619334013330	1905–1940	3.4	639	20	429	−34.0	−35.2
Shuram	OMR099	At	105518471651420	2379	1.5	NA	NA	NA	−37.0	−36.6
Shuram	OMR150	At	105518471651420	2053–2121	1.3	NA	NA	NA	−36.4	−36.7
Shuram	OMR151	At	105518471651420	2424.5–2447	3.0	NA	NA	NA	NA	−35.1
Shuram	OMR152	At	105518471651420	2449–2452	3.6	NA	NA	NA	−35.7	−35.0
Shuram	OMR154	Tu	105619363441090	2247.5–2249.6	NA	NA	NA	NA	NA	−38.2
Shuram	OMR155	Th	105518260443550	2350–2435	2.4	NA	NA	NA	−35.4	−37.2
Shuram	OMR156	Th	105518260443550	2685–2740	3.9	NA	NA	NA	−34.8	−34.7
Silicylite	OMR004	At	105518471651420	1198–1425	3.4	569	31	423	−35.9	−36.5
Silicylite	OMR012	Ma	105518120745470	2104–2120	3.4	550	36	424	−37.2	−37.4
Silicylite	OMR013	Ma	105518120745470	2240–2352	2.3	592	37	420	−37.1	−36.5
Silicylite	OMR023	Th	105517095822260	1551–1602	4.3	579	23	423	−36.9	−37.7
Silicylite	OMR024	Th	105517095822260	1628–1742	2.6	690	33	424	−35.6	−35.8
Thuleilat shale	OMR003	At	105518471651420	1000–1102	8.0	560	17	425	−36.2	−37.9
Thuleilat shale	OMR011	Ma	105518120745470	2068–2084	10.4	600	11	433	−36.3	−37.3
Thuleilat shale	OMR021	Th	105517095822260	1417.5–1483	6.4	574	21	429	−36.5	−38.1
Thuleilat shale	OMR022	Th	105517095822260	1520–1547	2.5	454	25	422	−37.1	−37.7
U shale	OMR005	At	105518471651420	1425–1527	3.5	337	26	419	−35.2	−35.6
U shale	OMR006	At	105518471651420	1527–1650	4.9	378	19	425	−35.3	−36.3
U shale	OMR007	At	105518471651420	1773–1872	5.7	312	22	430	−36.3	−37.6
U shale	OMR014	Ma	105518120745470	2420–2460	6.4	559	20	429	−34.3	−34.8
U shale	OMR025	Th	105517095822260	1751–1833	4.0	506	22	425	−33.9	−34.2

the Ara Group contains rocks of the Athel (Al Shomou) Silicilyte (TOC 3–4%; HI 400–700) and U shale formations (TOC 5–15%; HI 300–700) that are reputed to be 'world class' (Terken et al., 2001). A re-examination of Athel intra-salt rocks also identifies the Thuleilat Fm. as an excellent source rock, with TOC between 5 and 15% and HI values around 600 mg HC/g org. C on average. In the carbonate domains of the intra-salt section the occurrence of organic-rich horizons is limited. Typical TOC for carbonate stringers is around 1%. TOC values >1% in some carbonate stringers were found to be caused by the presence of migrated residual oil (Paul Taylor, personal communication), however the carbonate stringer rocks presented in this study do not show this character. Samples at the top salt A6C (Dhahaban Fm.) have values up to 8% and an HI average of 600, i.e. attributes of a high quality source rock (Terken and Frewin, 2000). A screening of pre-salt rocks revealed the occurrence of high quality, oil-prone source rocks in the Nafun Group, more particularly in the Lower and Upper Masirah Bay (TOC 1–10%; HI 400–700), the Lower and Upper Shuram (TOC 2–5%; HI 200–600) and the Buah (TOC 2%; HI 300–600) formations (Paul Taylor, personal communication). Those with the widest distribution are from the Lower Shuram and Upper Masirah Bay formations.

6. Source rock geochemistry

6.1. Bulk carbon isotopic composition

Bulk $\delta^{13}C$ values for the saturated and aromatic hydrocarbon fractions of the rocks show overall depleted values (Table 1), typical of Precambrian rocks (Andrusevich et al., 1998). The carbon isotopic character of hydrocarbons from the individual Huqf formations is fairly variable, in particular within the Nafun Group, oscillating between the relatively heavy values of the Masirah Bay Fm. (reaching −31‰ for saturates and aromatics) and the exceedingly light values of the Buah samples (ca.−39‰; Table 1). The saturated and aromatic hydrocarbon $\delta^{13}C$ values from the Thuleilat Fm. form a tight cluster around −37‰, whereas a fairly wide range of values (−34‰ to −37‰) is observed within the Shuram and U shale formations (Table 1). The saturates and aromatics of the Athel Silicilyte bitumens have values very close to those of the Thuleilat Fm, with an average of −36.5‰.

The lower carbonate stringers A1C and A2C exhibit $\delta^{13}C_{sats}$ and $\delta^{13}C_{aros}$ values slightly lighter than those of the upper horizons A3C–A5C (Table 1). Overall, the carbonate stringer hydrocarbons have slightly heavier average $\delta^{13}C$ values than the time-equivalent

Table 2
API data, bulk carbon isotopic composition and relevant MRM biomarker ratios for the oils. (Biodeg., biodegradation rank; PS Huqf, Post-salt Huqf oil; NA, not available. Biomarkers were measured from specific MRM transitions and the following ratios were calculated: 22T/21T = C_{22} tricyclic terpane/C_{21} tricyclic terpane; 24T/23T = C_{24} tricyclic terpane/C_{23} tricyclic terpane; GA/30H = gammacerane/C_{30} αβ-hopane; 35H/34H = (C_{35} αβ-hopanes 22*S* + 22*R*)/(C_{34} αβ-hopanes 22*S* + 22*R*); TNH/(Ts + Tm) = 25,28,30-trinorhopane/(Ts + Tm); DNH/30H = 28,30-dinorhopane/C_{30} αβ-hopane; 2MH/3MH = 2α-methyl C_{30} hopane/3β-methyl C_{30} hopane; 2MHI: 2-methylhopane index = 2-methyl C_{30} hopane/(2-methyl C_{30} hopane + C_{30} hopane) × 100).

Stratigraphy	MIT ID	Well ID	Field	Min. depth (m)	API	13δ Sats	136ATOS	Biodegr.	22T/21T	24T/23T	GA/30H	35H/34H	TNH/(Ts+Tm)	DNH/30H	2MH/3MH	2MHI
A1C	OMO005	105417294105520	DHAHABAN SOUTH	2926.1	51.7	−35.6	−35.7	0	0.3	0.39	0.15	1.73	0.02	0.23	1.74	6.74
A1C	OMO040	105518011119180	KAUKAB	3163	32.6	NA	−35.2	0	0.33	0.51	0.15	1.36	0.01	0.09	1.34	7.79
A2C	OMO033	105418330226010	SAKHIYA	4793	34.7	NA	−33.3	0	0.41	0.48	0.17	1.46	0.10	0.21	1.07	5.14
A2C	OMO034	105418380655030	RABAB	4356	48.5	−34.2	−33.7	0	0.44	0.49	0.17	1.37	0.07	0.14	1.00	4.85
A2C	OMO049	105417365600000	HARWEEL DEEP	3746.3	60	−35.7	−35.2	0	0.44	0.42	0.15	1.65	0.04	0.20	2.01	7.14
A2C	OMO053	105417295308420	GHAFEER	4330.04	37.1	−35.1	−34.4	0	0.41	0.40	0.16	1.56	0.06	0.16	1.29	5.66
A2C	OMO055	105418300002430	ZALZALA	4916	39.1	−34.2	−33.0	0	0.36	0.46	0.14	1.40	0.04	0.21	1.51	5.59
A2C	OMO056	105418340256100	FAYROUZ	4472	51.5	−34.9	−34.1	0	0.38	0.58	0.13	1.44	0.13	0.21	1.42	5.18
A2C	OMO057	105417295829310	DAFAQ	5096	39.8	−34.7	−34.0	0	0.36	0.48	0.17	1.46	0.04	0.13	1.49	6.47
A3C	OMO031	105417365600000	HARWEEL DEEP	311054	22.5	−35.2	−35.0	0	0.241	0.49	0.22	1.62	0.11	0.24	1.46	7.41
A3C	OMO039	105418591443090	DURRA	2952.6	35	−34.8	−34.6	0	0.43	0.39	0.22	1.81	0.20	0.28	1.92	7.76
A3C	OMO041	105518011119180	KAUKAB	2779.5	29.1	−35.0	−34.9	0	0.45	0.39	0.21	1.89	0.23	0.26	1.84	7.63
A3C	OMO051	105417355604421	SARMAD	3651	32.6	−35.4	−35.2	0	0.39	0.45	0.19	6.71	0.10	0.18	1.47	6.71
A3C	OMO052	105417275338150	GHAFEER	4339	35.7	−34.9	−34.0	0	0.41	0.43	0.17	1.56	0.03	0.09	1.24	5.62
A4C	OMO006	105518042847200	BIRBA NORTH	3680.8	50	−34.9	−34.7	0	0.46	0.43	0.19	1.77	0.15	0.24	1.99	8.51
A4C	OMO016	105518061802480	BIRBA	2790.4	30.5	−34.7	−34.7	0	0.45	0.43	0.24	1.97	0.20	0.33	1.61	8.12
A4C	OMO036	105518061721330	BIRBA SOUTH	2576.78	46.8	−34.5	−34.8	0	0.42	0.41	0.19	1.72	0.26	0.31	1.82	8.04
A4C	OMO038	105518051934160	BIRBA	2832.81	28	−34.4	−34.8	0	0.38	0.39	0.21	1.76	0.24	0.32	1.87	8.06
A4C	OMO058	105518052416051	BUDOUR	3219	51.5	−35.2	−34.9	0	0.41	0.41	0.16	1.62	0.31	0.38	2.64	10.24
A4C+A3C	OMO045	105518022220500	OMRAAN	3178.1	30.9	−34.7	−34.7	0	0.39	0.40	0.20	1.79	0.19	0.31	1.71	7.29
A5C	OMO015	105620080139160	SU WAI HAT	3715.8	49.7	−35.9	−34.5	0	0.50	0.38	0.14	1.98	0.02	0.15	2.66	9.21
A5C	OMO037	105518022220500	OMRAAN	2840.13	30.7	−34.8	−34.6	0	0.40	0.42	0.22	1.77	0.20	0.31	2.07	8.22
A5C	OMO043	105418430658140	HAWMYAT	3933	28.2	−34.6	−34.7	0	0.30	0.53	0.12	1.30	0.49	0.16	2.56	8.09
A5C	OMO054	105417335655201	SARMAD	3742	33.4	−35.2	−34.8	0	0.39	0.43	0.18	1.65	0.10	0.19	1.68	7.56
A6C	OMO035	105418330316080	ANDHUR	3442.72	28.3	−34.8	−34.3	0	0.43	0.41	0.19	1.61	0.12	0.21	1.81	8.18
A6C	OMO059	105417205122490	QASHOOB	4819	32.3	−36.1	−35.7	0	0.26	0.59	0.17	0.98	0.06	0.30	1.74	9.57
PS Huqf	OMO002	105619282116100	MUKHAIZNA NORTH	844.3	16.3	−35.4	−35.7	1	0.59	0.36	0.21	2.89	0.1	0.19	1.79	8.15
PS Huqf	OMO003	105417263411030	JAZAL	878.1	27.8	−33.9	−34.1	0	0.49	0.38	0.20	1.98	0.10	0.20	0.79	4.94
PS Huqf	OMO004	105518574204450	NIMR	880.9	biodegraded	−35.4	−36.0	4	0.01	0.151	0.15	1.71	0.01	0.15	1.52	7.04
PS Huqf	OMO007	105619260135090	JALMUD NORTH	1060.7	25.9	−34.8	−35.6	0	0.44	0.46	0.16	1.99	0.01	0.06	1.81	7.39
PS Huqf	OMO008	105618074334180	RUNIB	795.5	25	−36.2	−36.2−36	1	0.41	0.49	0.151	1.60	0.1	0.15	1.61	5.50
PS Huqf	OMO009	105618164010550	NUWAR	1497.8	1497.81	−35.8	−36.7	2	0.58	0.33	0.26	2.0	0.03	0.19	2.09	10.08
PS Huqf	OMO010	105518160817390	MARMUL	894.3	22.1	−35.5	−35.9	1	0.45	0.45	0.20	2.03	0.01	0.19	1.67	8.34
PS Huqf	OMO011	105518533910250	NIMR	929.6	20.6	−35.2	−35.7	4	0.41	0.01	0.12	1.55	0.01	0.12	1.68	6.43
PS Huqf	OMO013	105618204222150	SAHAM	1059.2	3.4	−35.3	−36.1	2	6.1	0.48	0.26	1.84	0.02	0.14	1.40	10.24
PS Huqf	OMO014	105619001739100	GHUFOS	1131.4	28.1	−36.1	−36.7	1	0.68	0.31	0.42	2.59	0.04	0.24	2.00	13.56
PS Huqf	OMO022	105518260537100	THAMOUD	1385	biodegraded	−35.9	−36.1	0	0.54	0.39	0.22	1.82	0.04	0.23	2.18	9.72
PS Huqf	OMO023	105618164728380	REIHAN	1312	21	−35.7	−36.4	1	0.51	0.46	0.14	1.77	0.02	0.09	1.48	6.37
PS Huqf	OMO024	105518140623080	MARMUL	915.3	21.4	−35.8	−35.9	0	0.52	0.44	0.21	1.79	0.01	0.20	1.88	9.48
PS Huqf	OMO026	105518271257290	MAURID	1129	biodegraded	−35.7	−35.9	1	0.61	0.36	0.26	1.99	0.02	0.30	2.40	10.36
PS Huqf	OMO028	105618305524220	THURAYAH	1438	13.7	−35.0	−36.9	0	0.58	0.33	0.21	2.16	0.01	0.06	1.80	6.89

Q	OMO001	10551952185313O	MISFAR	600.5	biodegraded	−30.3	−30.6	0	0.27	0.79	0.78	0.19	0.12	0.76	0.24	4.27
Q	OMO012	10562008013916O	SU WAI HAT	1708.4	41	−31.8	−31.4	0	0.29	0.74	0.65	0.4	0.08	0.48	0.44	5.77
Q	OMO018	10562020314013O	ANZAUZ	1951.2	45.8	−32.4	−31.8	4	0.36	0.720	0.61	1.78	0.12	0.72	0.50	5.48
Q	OMO019	10552055212851O	ZAULIYAH	2304	43.5	−31.2	−30.9	0	0.32	0.81	0.84	1.76	0.08	0.96	0.26	3.65
Q	OMO020	10561900422611O	KATHEER	1273	41.8	−31.3	−31	0	0.28	0.79	0.56	1.47	0.09	0.74	0.31	3.30
Q	OMO021	10561900173910O	GHUFOS	930.2	28.3	−30.5	−30.7	4	0.28	0.76	0.81	1.68	0.14	1.07	0.36	5.04
Silic.	OMO025	10551829411341O	AL NOOR	4258	46.9	−35.1	−34.9	0	0.54	00.540	0.20	2.581	0.01	0.12	2.58	12.08
Silic.	OMO029	10551825382732O	ALSHOMOU	3653.3	51.5	−34.4	−34.1	0	0.38	0.38	0.25	1.34	0.04	0.20	NA	12.01
Silic.	OMO030	10551828414744O	AL NOOR	4239	45.6	−34.7	−34.9	0	0.49	0.41	0.18	1.48	02.11	0.10	2.11	11.07
Silic.	OMO044	10551829414038O	AL NOOR	3992	47.3	−35.4	−35.5	0	0.49	0.41	0.18	1.54	0.01	0.13	2.09	10.99
Silic.	OMO046	10551825384727O	ALSHOMOU	3771	46.5	−33.7	−33.8	0	0.39	0.42	0.23	1.91	0.01	0.12	2.29	9.71
Silic.	OMO048	10551825384727O	ALSHOMOU	4023	condensate	−36.4	−34.7	0	0.2	0.2	0.24	1.92	0.02	0.11	1.98	10.70
Silic.	OMO050	10551829412927I	AL NOOR	4081	47.2	−35.3	−35.4	0	0.49	0.41	0.18	1.61	0.1	0.11	2.26	10.92

Athel intra-salt bitumens. This difference has been attributed to a shallower water column over the platform limiting carbon assimilation and, therefore, leading to less ^{13}C depletion (Gelin et al., 1999).

6.2. Molecular composition

Biomarker ratios measured from specific MRM transitions are given for each individual rock sample as supplementary information in Table S1. Averaged ratios for each formation are shown in Table 3.

6.2.1. Normal and branched alkanes

GC traces of the alkane fractions from representative rock samples are shown in Fig. 3. Pr/Ph values are well below 0.8, with the exception of Masirah Bay sample OMR027 and Buah sample OMR020. These low values reflect anoxic conditions during deposition as well as saline to hypersaline conditions associated with carbonate and evaporite deposition (Peters et al., 2005). All Huqf Supergroup rocks contain characteristic mid chain MMAs (originally designated X-compounds; Grantham et al., 1987) and their relative abundance is enhanced in the range C_{20}–C_{24} and drops significantly above C_{24} (Fig. 3). However, on average, mid chain MMAs tend to be relatively more abundant in Ara samples than in the Nafun rocks (Fig. 3 and Table 3). The exact origin of these branched alkanes is uncertain. A bacterial source has been suggested, as mid-chain methyl alkanes are present in cyanobacteria (Gelpi et al., 1970; Paoletti et al., 1976) and modern cyanobacterial mats (de Leeuw et al., 1985; Robinson and Eglinton, 1990). Mid-chain branched fatty acids in symbiotic bacteria living in sponges are also potential precursors (Thiel et al., 1999). However, none of these modern precursors gives rise to distributions exactly comparable to those in Oman bitumen and kerogen pyrolyzates in terms of chain length and branching loci (Höld et al., 1999), leaving open the question of their source.

6.2.2. Steranes

Sterane distributions in Huqf rocks present numerous features peculiar to rocks of such age. One of the most distinctive characteristics is the predominance of C_{29} steranes, constituting on average 70% of the C_{27}–C_{29} steranes for all the Huqf rock samples. It is remarkable that this feature occurs throughout the Huqf Supergroup from the Masirah Bay Fm. rocks at the base of the Nafun to near the top of the Ara Group (Fig. 4a) in the A5 stringer. Such C_{29}-sterane dominated distributions have been observed in Neoproterozoic geological samples worldwide (Fowler and Douglas, 1987; Summons and Powell, 1992; Peters et al., 1995) and are attributed to green algae (Grantham and Wakefield, 1988), which synthesize primarily C_{29} steroids (Volkman, 2003) and must have been important primary producers at the time. The broad age distribution of C_{29} sterane dominance even extends down into the glaciogene Ghadir Manqil Fm. (data not shown). This unit most likely predates the Acraman impact event in Australia and first appearance of abundant C_{29} steranes recorded in sediments of the Centralian Superbasin (McKirdy et al., 2006).

The C_{29} sterane predominance aside, sterane distributions across the Huqf Supergoup share other remarkable features. The C_{30} desmethylsterane distributions are characterized by the concomitant presence of 24-*n*-propylcholestanes and 24-isopropylcholestanes in all Huqf rock samples (Fig. 5). Empirical data suggest 24-*n*-propylcholestanes are derived from marine chrysophyte algae and are diagnostic for marine depositional environments (Moldowan et al., 1990). On the other hand, 24-isopropylcholestanes have been shown to predominate over 24-*n*-propylcholestanes in Late Proterozoic and Early Cambrian sediments and oils, which is hypothesized to reflect the radiation

Table 3
Averages of relevant MRM biomarker ratios for each Huqf formation. Refer to Table 2 for biomarker ratios (X-22: mid-chain C_{22} MMAs; *n*-22: linear C_{22} alkane; Tet = C_{24} tetracyclic terpane).

Formation	DNH/30H	TNH/(Ts + Tm)	DNH/TNH	35H/34H	GA/30H	21-nor/27-nor[a]	X-22/*n*-22	X-24/*n*-24	2MH/3MH	2MHI	29dia/st[b]	22T/21T	24T/23T	Tet/23T	Sterane/Hopane[c]	19A (μg/g TOC)	19B (μg/g TOC)	19C (μg/g TOC)
Masirah Bay	0.05	0.01	6.77	1.09	0.09	0.09	0.30	0.35	1.45	5.42	0.08	0.25	0.47	0.25	0.66	0.34	1.24	0.09
Shuram	0.08	0.02	5.52	1.52	0.14	0.12	0.62	0.65	2.54	9.50	0.06	0.46	0.46	0.30	0.79	0.43	1.84	0.09
Shuram w/out anomalies	0.07	0.02	4.84	1.42	0.12	0.09	0.45	0.48	2.14	7.17	0.07	0.34	0.56	0.27	0.71	0.35	1.46	0.07
Buah	0.09	0.02	7.19	1.58	0.14	0.09	0.67	0.36	1.01	6.27	0.16	0.42	0.43	0.45	0.85	0.17	0.82	0.03
Buah w/out anomalies	0.06	0.03	4.60	1.47	0.06	0.06	0.51	0.30	0.84	3.69	0.21	0.35	0.50	0.48	0.78	0.12	0.45	0.02
Nafun	0.08	0.02	6.21	1.43	0.13	0.10	0.56	0.51	1.93	7.78	0.09	0.40	0.45	0.32	0.77	0.34	1.42	0.07
Nafun w/out Shuram/Buah anom.	0.06	0.02	5.48	1.31	0.09	0.08	0.41	0.39	1.54	5.58	0.11	0.31	0.51	0.32	0.71	0.28	1.09	0.06
U shale	0.20	0.11	3.49	1.62	0.11	0.11	0.77	0.60	2.43	7.65	0.03	0.68	0.31	0.22	0.89	0.22	1.07	0.06
Silicilyte	0.78	1.46	1.34	1.93	0.18	0.06	0.98	1.12	3.45	11.85	0.02	0.79	0.27	0.22	1.08	0.37	2.01	0.08
Thuleilat shale	0.75	0.45	1.94	2.00	0.21	0.08	0.64	0.67	2.78	11.89	0.03	0.80	0.24	0.25	0.91	0.16	0.89	0.03
Athel intra-salt	0.56	0.69	2.28	1.84	0.16	0.08	0.81	0.81	2.90	10.36	0.03	0.76	0.28	0.23	0.96	0.25	1.31	0.05
Carbonate stringers	0.27	0.16	4.61	1.77	0.23	0.19	0.46	0.46	1.68	7.98	0.03	0.46	0.41	0.22	0.89	0.45	2.69	1.25
Ara total (Athel & carbonate stringers)	0.41	0.41	3.49	1.80	0.19	0.14	0.81	0.81	2.26	9.13	0.03	0.60	0.35	0.23	0.93	0.36	2.05	0.70

[a] 21-nor/27-nor = 21-norcholestane/(27-norcholestanes ααα + αββ).
[b] 29 dia/st = C_{29} βα diasteranes/(ααα + αββ steranes).
[c] Steranes/Hopanes = Sum (C_{27}–C_{29} βα diasteranes, ααα and αββ steranes)/Sum (C_{27}–C_{35} hopanes).

of sponges, as their sterol precursors occur in sponges of the class *Demospongiae* (McCaffrey et al., 1994). Huqf rocks show 24-isopropylcholestanes/(24-isopropyl + 24-*n*-propylcholestanes) proportions varying between 36% and 94%, with a total average of 58% for the whole set of rocks (Fig. 4b).

C_{26} steranes, occurring as both 27-norcholestanes and 21-norcholestane and excluding 24-norcholestanes (Fig. 5), comprise a large proportion (on average 6%) of the total C_{26}–C_{29} steranes and likely reflect a combination of biological inputs specific to this period of time. Relative concentrations of 21-norcholestane have been shown to increase with maturity (Moldowan et al., 1991) but may also be related to OM deposition under hypersaline conditions (Guzmán-Vega et al., 1997). The relative abundance of 21-norcholestane vs. 27-norcholestanes is the highest for carbonate stringers (Table 3).

C_{30} ring-A methyl sterane distributions are largely dominated by 3β-methylstigmastanes in all the Huqf rocks (Fig. 5). This preponderance over methyl steranes alkylated at C-2 and C-4 is characteristic of Late Proterozoic and Paleozoic geological samples (Summons and Powell, 1987, 1992). However, it is also significant that trace levels of 4-methylsteranes, including dinosteranes and 24-ethyl-4-methylcholestanes were identified in all the samples and there is no evidence to suggest that their presence is due to contamination from geologically younger hydrocarbons.

Sterane distributions are fairly similar across the different Huqf formations and the main distinctive feature is a low diasterane content in Ara rocks (Fig. 5 and Table 3), which are carbonates, or otherwise starved of clastic input, compared to the Nafun samples which are from a predominantly clastic sequence. This accords with observations for much younger petroleum provinces such as those of the California Borderland basins (Brincat and Abbott, 2001).

6.2.3. Hopanes

The distributions throughout the Huqf Supergroup are generally characterized by relatively high C_{35} hopane abundance (Fig. 6), as illustrated by the averaged C_{35} hopane/C_{34} hopane (35H/34H) values in Table 3. However, compared to Nafun rock samples, Ara samples (Athel intra-salt rocks and carbonate stringers included) display, on average, higher C_{35}/C_{34} hopane values, consistent with more reducing depositional conditions (Peters and Moldowan, 1991). Highly reducing environments are also suggested by the substantial content of 28,30-dinorhopane (DNH) and 25,28,30-trinorhopane (TNH) in these rocks. These two compounds, typical of petroleum source rocks deposited under anoxic, or euxinic, conditions (Curiale et al., 1985; Mello et al., 1988; Brincat and Abbott, 2001), are best detected and quantified using the MRM transitions 384 → 191 Da and 370 → 177 Da (Fig. 6). Within the intra-salt section, ratios of 28,30-dinorhopane to C_{30} hopane (DNH/30H) and TNH/(Ts + Tm), used to assess the relative abundances of 28,30-dinorhopane and 25,28,30-trinorhopane, are by far the highest in the Athel Silicilyte and Thuleilat Fm. samples, whereas they appear to be at an intermediate level in the U Shale Fm. and carbonate stringers (Fig. 7a). The silicilyte samples show the highest absolute abundances for DNH and TNH, culminating at 77 and 176 ng/g TOC, respectively. In contrast, ratios DNH/30H and TNH/(Ts + Tm) are extremely low for all Nafun bitumens (Table 3). Unfortunately, although 28,30-dinorhopane and 25,28,30-trinorhopane discriminate the Nafun rock samples from the Ara samples quite remarkably, their application in oil-source correlation has been limited due to their high sensitivity to maturity. They are thought not to be bound to the kerogen, occurring rather as free hydrocarbons (Noble et al., 1985) and, as a consequence, their relative abundance tends to diminish markedly with increasing maturity (Moldowan and Seifert, 1984). The fact that 28,30-dinorhopane and 25,28,30-trinorhopane did not appear to be incorporated into kerogen led

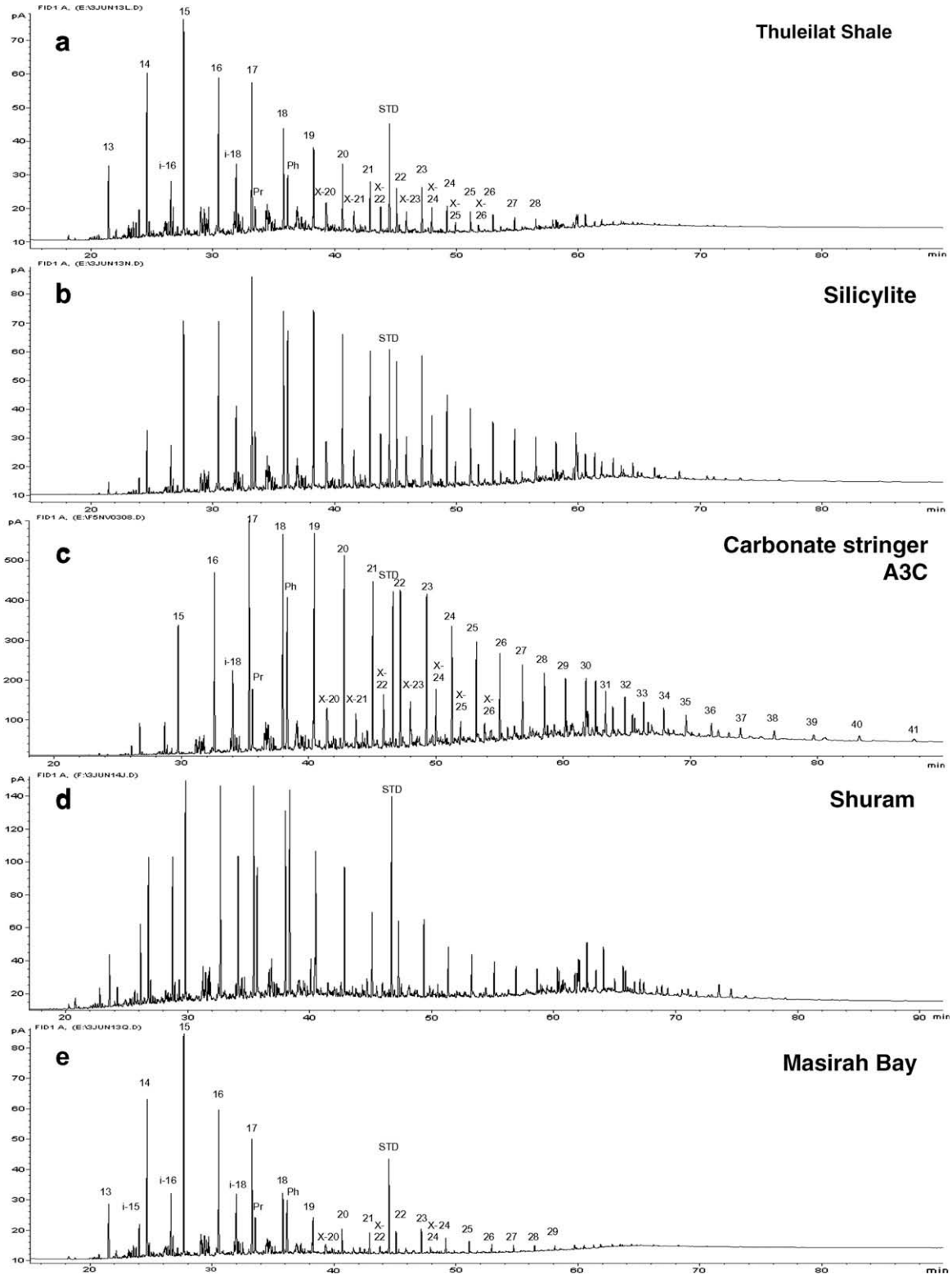

Fig. 3. GC traces of total alkanes of representative rocks: (a) Thuleilat Shale, (b) Silicilyte, (c) Carbonate Stringer (CS) A3C, (d) Shuram and (e) Masirah Bay. Linear alkanes are indicated by their carbon number. Each X-peak represents coelution of several MMAs branched at different positions: e.g. X-24 is a mixture of 11- and 12-methyltricosane. STD, internal standard 3-methylheneicosane; Pr, pristane; Ph, phytane; i-16, C_{16} isoprenoid alkane.

to the suggestion they are products of early diagenetic bacterial reworking (Curiale et al., 1985) and possibly synthesized by sulfur oxidizing bacteria (Williams, 1984).

Gammacerane, a biomarker for water column stratification commonly induced by hypersalinity (Moldowan et al., 1985; Sinninghe Damsté et al., 1995), is present in all the Huqf rock bitumens but tends to be in greater proportion in Ara samples than in Nafun rocks and, in particular, in carbonate stringers, the Athel silicilyte and the Thuleilat shale, suggesting elevated salinity in the original water column for these rocks (Fig. 7b).

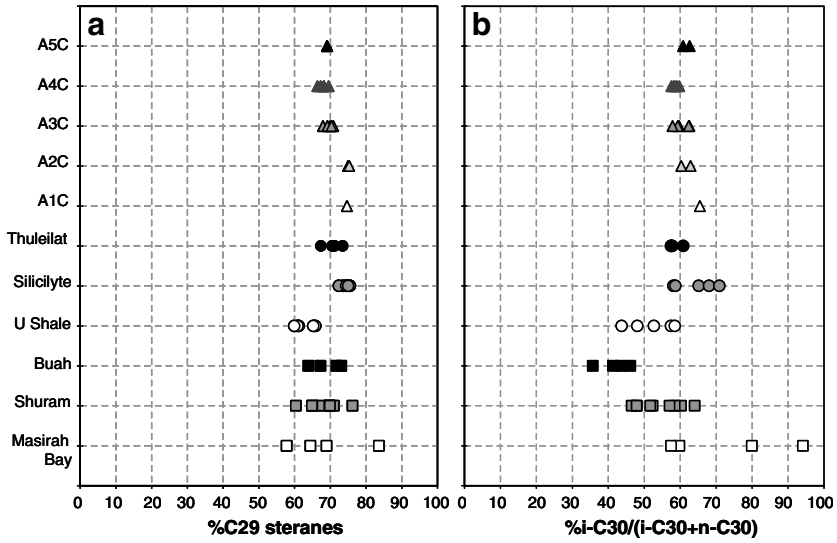

Fig. 4. (a) % C_{29} steranes and (b) % *i*-C30/(i-C30 + *n*-C30) for all Huqf rock formations. % C_{29} steranes = [C_{29} βα diasteranes, ααα and αββ steranes]/[(C_{27} + C_{28} + C_{29}) βα diasteranes, ααα and αββ steranes] × 100. % *i*-C30/(*i*-C30 + *n*-C30) = 24-isopropylcholestanes (ααα + αββ)/[(24-isopropyl- + 24-*n*-propylcholestanes) (ααα + αββ] × 100.

C_{31} to C_{36} A-ring methylated hopanes are present in Huqf rocks as 2α-methylhopanes and 3β-methylhopanes (Fig. 6). Proportions of 2α-methylhopanes relative to 3β-methylhopanes vary quite significantly among Huqf rock samples: the Masirah Bay and Buah formations show the highest 3β-methylhopane to 2α-methylhopane ratio values (Fig. 7c), whereas they are lowest for the Ara samples from the silicilyte and the Thuleilat Fm. and for some pre-salt Shuram rock samples. On average, the ratio of 2α-methylhopanes to 3β-methylhopanes for all Ara samples is 2.3, as opposed to 1.9 for Nafun samples (Table 3). An inversely proportional trend is observed for the 2α-methylhopane index (2-MHI = C_{30} 2-methylhopane/(C_{30} 2-methylhopane + C_{30} hopane)), a potentially useful tracer for cyanobacterial input to sedimentary OM (Summons et al., 1999).

6.2.4. Cheilanthanes

Huqf bitumens contain tricyclic terpanes (cheilanthanes) with C_{23} predominant. However, distributions across the respective formations are variable, as shown by C_{22} tricyclic terpane/C_{21} tricyclic terpane (22T/21T), 24T/23T (Fig. 7d) and 26T/25T ratios. On average, Athel intra-salt rocks show high 22T/21T combined with low 24T/23T values, whereas the opposite trend is observed for most of the Nafun rocks, with some exceptions in the Shuram and Buah formations. Carbonate stringer samples have values intermediate between these two end members (Fig. 7d). The relative proportion of the C_{24} tetracyclic terpane when compared to cheilanthanes also fluctuates across the Huqf Supergroup, with values of C_{24} tetracyclic to C_{23} tricylic slightly higher in Nafun rocks than Ara intra-salt rocks (Table 3).

6.2.5. Aromatic hydrocarbons

Aromatic fractions were analyzed using GC–MS with selected ion monitoring in order to target specific compound classes such as aromatic steroids, aromatic hopanoids and aryl isoprenoids. Monoaromatic, triaromatic and methyl triaromatic steroids and benzohopanes were detected but none were useful in distinguishing Nafun from Ara rocks. In particular, the ratio of 3-methyl/4-methyl C_{29} triaromatic steroid developed in previous unpublished studies by Kohnen and Nederlof (Paul Taylor, personal communication) did not confirm its potential as a discriminating parameter given that we found there was significant overlap in this parameter between Ara and Nafun rocks.

Despite a concerted search, the diaryl isoprenoid isorenieratane, derived from anoxygenic photosynthetic sulfur bacteria (Chlorobiaceae) and therefore often associated with euxinic basins (Brocks and Summons, 2003), was not detected in any aromatic fractions, including Raney Ni-desulfurised aromatic fractions and hydropyrolysis products. However, short chain 2,3,6-aryl isoprenoids (along with 2,3,4-) could be found in trace levels. The significant concentrations of 28,30-dinorhopane and 25,28,30-trinorhopane in Ara rocks, together with relatively high abundances of C_{35} hopanes and gammacerane, all indicate that these rocks were deposited in a periodically or permanently stratified basin characterized by anoxic or euxinic bottom waters. On the other hand, evidence from the patterns of sulfur isotopes in coeval pyrite and carbonate-associated sulfate in the Huqf sediments shows that the ocean feeding water into the restricted environment of the SOSB became progressively oxygenated during the deposition of the entire Nafun Group (Fike et al., 2006).

6.3. Ara versus Nafun geochemical character: summary

One of the aims of this study was to identify geochemical attributes discriminating the Nafun sediments from the Ara sediments in order to better understand and predict their respective contributions to the oil accumulations. To achieve this goal, the selection of a reliable and pristine sample set was absolutely critical and extreme care was taken regarding the choice of the rocks. However, during the course of the study, it became clear that contamination of Huqf rocks and, in particular, some from the Nafun Group, was a cause for concern. Several samples had to be removed from the initial Nafun set due to contamination with Phanerozoic hydrocarbons, most likely from drilling fluids used during coring (Stalvies, personal communication). While Phanerozoic staining of Huqf rocks is relatively easy to identify thanks to their distinct hydrocarbon biomarker assemblages, cross contamination between different Huqf formations, if it occurs, is obviously a much more subtle problem to pinpoint.

Several Nafun rocks from the Shuram and Buah formations (OMR149, OMR150, OMR099 from well At; OMR154 from well Tu; OMR155 from well Th) display features very similar to Ara intra-salt rocks (Fig. 7 and Table S1) and consequently, unique characteristics for these formations are extremely difficult to identify. Several possible explanations could account for these data including:

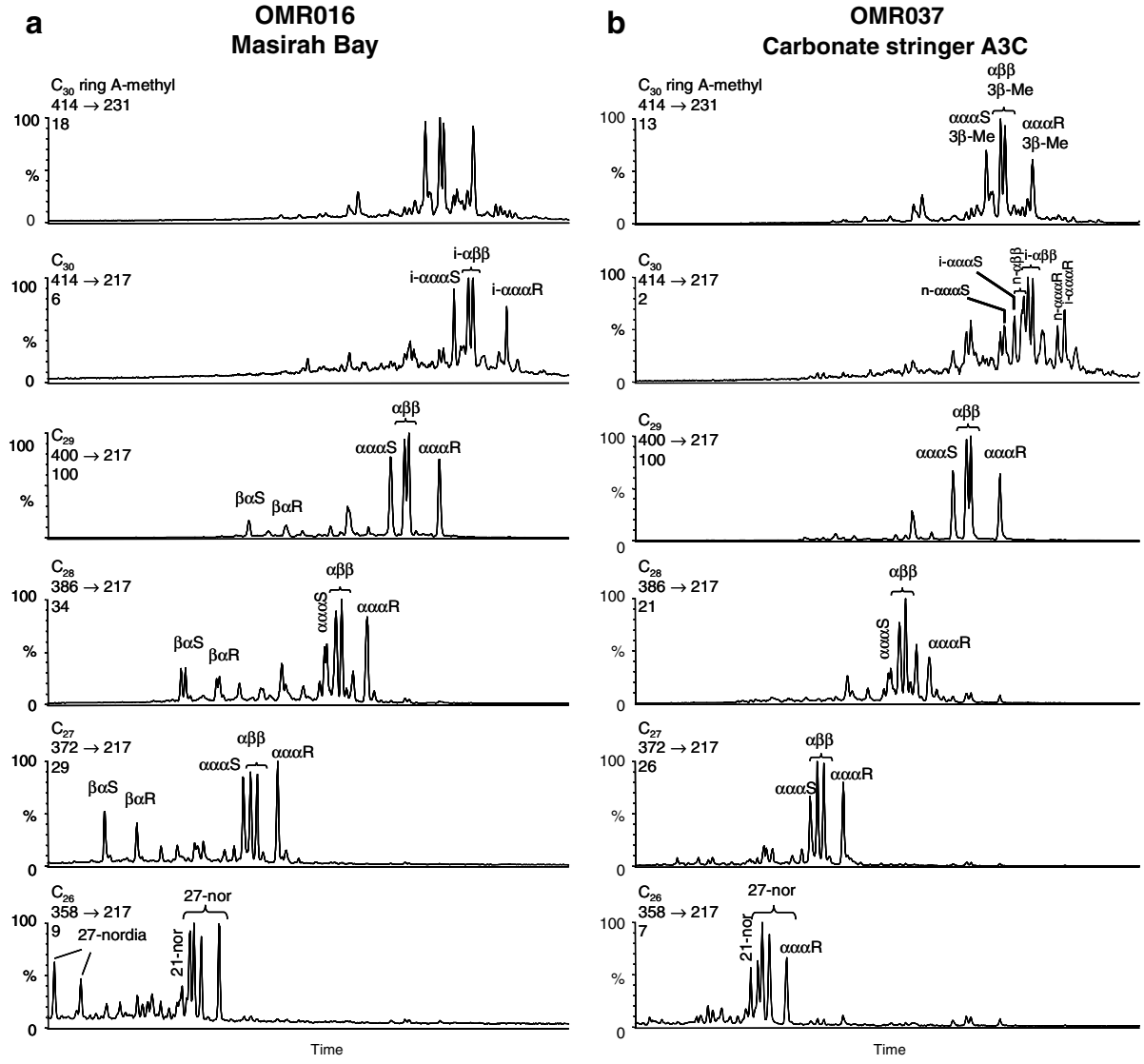

Fig. 5. MRM chromatograms showing distributions of C_{26}–C_{30} steranes of (a) Masirah Bay OMR016 and (b) CS rock A3C OMR037 (carbon number, specific transition and relative intensity shown). βα, ααα and αββ denote 13β (H),17α (H)-diasteranes, 5α (H),14α (H),17α (H)- and 5α (H),14β (H),17β (H)-steranes, respectively. *S* and *R* define the stereochemistry at C-20. 21-nor: 21-norsterane; 27-nor: 27-norsteranes; 27-nordia: 27-nordiasteranes; *n*- and *i*- in 414 → 217 Da indicate *n*-propylcholestanes and isopropycholestanes, respectively. 3β-Me in 414 → 231 Da denotes 3β-methylsteranes.

(1) These particular Nafun samples were compromised by caving of cuttings from organic-rich Ara units higher in the section during drilling of wells At, Th and Tu, or low angle faulting led to structural repetition of the Ara Fm. in these wells.
(2) They represent intersection of Ara-like facies in the Nafun that preceded their wider appearance in the overlying unit.

At this point, we cannot resolve these, although we note that deeper Nafun rocks from wells At (OMR152, 2449 m) and Th (OMR156, 2685 m and OMR157, 2895 m) do not show Ara characteristics. Hydropyrolysis of kerogens of the suspicious Shuram and Buah rocks would be needed in order to decipher whether cross-contamination effectively happened or not. A structural repeat and thickening of the Thuleilat–Silicilyte–U Shale package due to low angle faulting could also account for some of the observed inconsistencies. A close examination of the At well log suggests that samples identified as Shuram (OMR150 and OMR099) and Buah (OMR149) do not show the lithological, geochemical and well log attributes typical of these formations, raising doubts about the validity of these particular stratigraphic assignments. Indeed, Buah in well At presents a clastic lithology rather than being a carbonate unit and the Shuram unit does not display the generic negative carbon isotopic excursion.

Despite the incoherencies observed in the Shuram and Buah biomarker character, trends opposing Ara and Nafun rocks can be clearly identified when average values of parameters within respective formations are considered (Table 3). The geochemical characteristics that delineate Ara source rocks include: low Pr/Ph values; high relative abundance of mid-chain MMAs; high C_{35} hopanes/C_{34} hopanes, high relative abundance of gammacerane, 28,30-dinorhopane, 25,28,30-trinorhopane and 2-methylhopanes; low diasteranes; cheilanthanes ratios 22T/21T > 0.35 and 23T/24T < 0.50. In contrast, the geochemical attributes characterizing Nafun Group OM are: low abundance of mid-chain MMAs; low value for C_{22}/C_{21} tricyclic terpanes combined with elevated value of C_{24}/C_{23} tricyclic terpanes; low 2-methylhopane index combined with higher 3-Me/2-Mehopane ratio; low abundances of 21-norsteranes; low gammacerane/C30 hopane ratio; elevated

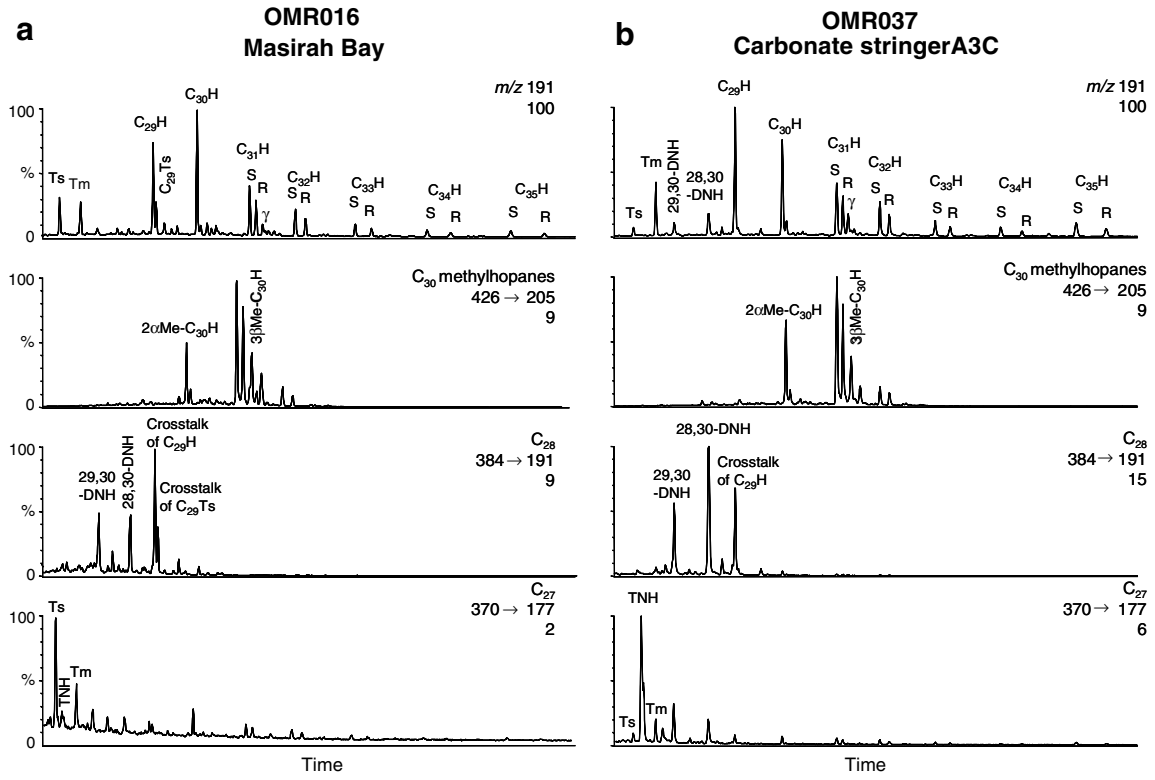

Fig. 6. MRM chromatograms showing 370 → 177, 384 → 191, 426 → 205 Da transitions and *m/z* 191 SIM chromatotogram for (a) Masirah Bay OMR016 and (b) CS rock A3C OMR037 (carbon number, specific transition and relative intensity shown). H: αβ-hopane; DNH: dinorhopane;γ: gammacerane; TNH: 25,28,30-trinorhopane; 2α-Me-C_{30}H: 2α-methyl C_{30} hopane. *S* and *R* define the stereochemistry at C-22.

abundances of the C_{24} tetracyclic terpane and diasteranes compared to Ara Group sediments.

Ara characteristics are particularly pronounced for the Athel Silicilyte and Thuleilat Fm. samples, whereas Nafun biomarker character is best represented in the Masirah Bay samples. Carbonate stringer rocks and U Shale samples appear, on average, to stand in between these two end members. These contrasts between Ara and Nafun group sediments are accentuated when the suspicious Shuram and Buah are removed from consideration, as shown by averages of parameters excluding these samples in Table 3.

6.4. Novel biomarkers in Huqf rock samples

Tetracyclic compounds characterized by a base peak at *m/z* 203 in their mass spectra occur pervasively in the alkane fractions of Oman rock samples. Molecular ions $M^{+\cdot}$ at *m/z* 260, 274 and 358 indicate the occurrence of C_{19}, C_{20} and C_{26} series respectively. The C_{19} components are readily detected using either MRM or SIM GC–MS, whereas the C_{20} and C_{26} homologues are better detected using the specificity of MRM analysis by means of the transitions 274 → 203 Da and 358 → 203 Da, respectively. The mass spectra are similar to those of steranes, with the *m/z* 217/218 shifted to *m/z* 203/204 and *m/z* 149 to *m/z* 135 (Fig. 8). Although further research is needed to rigorously establish the structures of these compounds, their diagnostic and common fragment ions at *m/z* 203 and 135 suggest that they are norsteranes missing a methylene unit from the A ring, whether by loss of the angular methyl or contraction of the ring, i.e. either 19-norsteranes or A-norsteranes respectively. Sedimentary A-norsteranes have been reported only rarely. C_{26}–C_{28} A-norsteranes were detected in Cretaceous black shales of Italy (van Graas et al., 1982) and structural studies revealed that they contained a steroid-based skeleton with a five carbon A-ring. Interestingly, and perhaps significantly in this case, A-ring contraction is a feature of sterols in some sponges (Minale and Sodano, 1974; Bohlin et al., 1980, 1981). Short chain A-norsteranes have, however, never been described. For simplification and clarity purposes, we name hereafter these tetracyclic compounds A-norsteranes, although this structural assignment requires proof.

While A-norsteranes were detected in all the Oman rocks, particular isomers within C_{19}, C_{20} and C_{26} A-norsterane distributions appear to be specific to the carbonate stringer rocks. In the alkane fractions of carbonate stringer bitumens, the distributions of C_{19} A-norsteranes, revealed by *m/z* 203 chromatograms, show three different isomers denoted 19A, 19B and 19C with the relative abundance 19B > 19C > 19A (Fig. 9a). Importantly, this pattern is also observed in the hydropyrolyzates of the carbonate stringer rocks (Fig. 9b), implying that these compounds are covalently bound to the kerogen and so cannot be attributed to staining or migration contamination. A systematic analysis of A-norsteranes in the free and kerogen-bound aliphatic fractions of other Huqf source rock facies (Stalvies et al., unpublished results) shows that the 19C isomer is virtually absent from Nafun rock samples (Masirah Bay, Shuram and Buah Fm.; Fig. 10a) as well as from Athel Basin intra-salt rocks (i.e. U Shale Fm./Athel Silicilyte/Thuleilat Fm.; Fig. 10b). Concentrations of the C_{19} A-norsteranes 19A, 19B and 19C normalized to TOC were calculated for bitumens from carbonate stringers, Nafun Group and Athel Intra-salt source rocks (Tables S1 and 3). Averaged abundances clearly show that isomers 19A and 19B are of the same order of magnitude across the whole sample set, whereas the distinctive 19C isomer is about 10 times more abundant in carbonate stringer rocks than in Nafun and Athel intra-salt rocks. Similarly, specific isomers of C_{20} and C_{26} A-norsteranes exclusively occur in carbonate stringer bitumens and are essentially absent from Nafun and Athel intra-salt rock samples (Fig. 11).

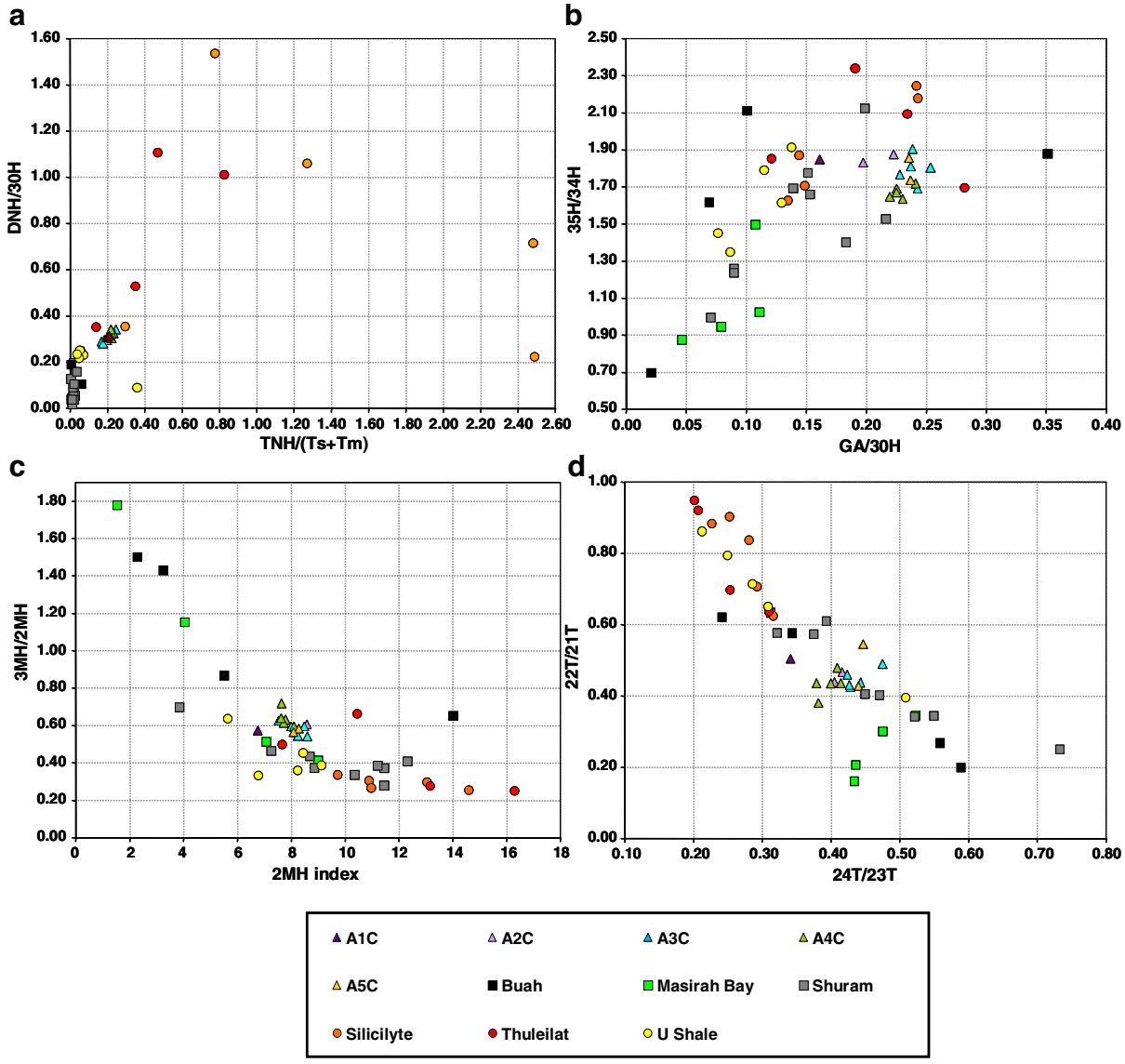

Fig. 7. Crossplots of selected biomarker ratios for Huqf source rocks. Refer to Table 2 for biomarker ratios.

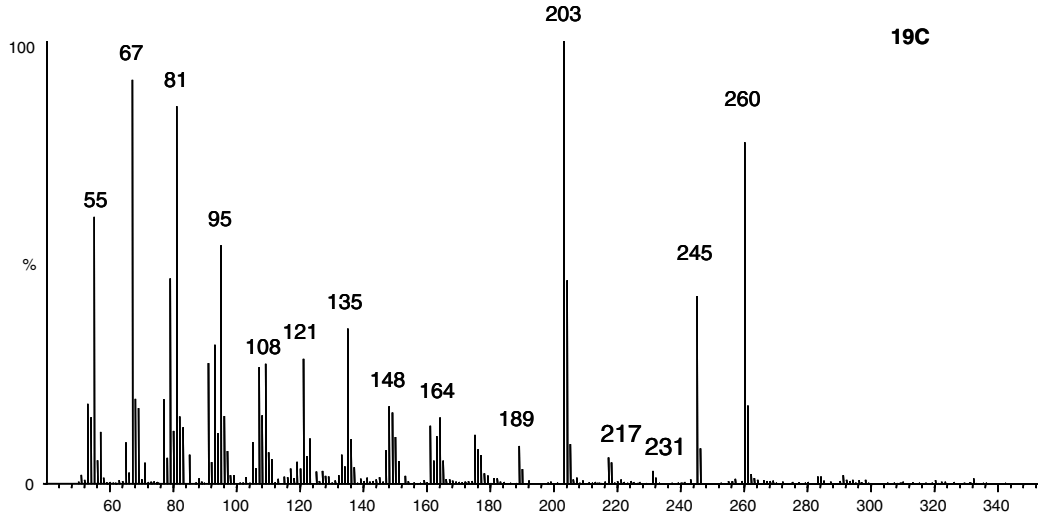

Fig. 8. Mass spectrum of putative C_{19} A-norsterane 19C.

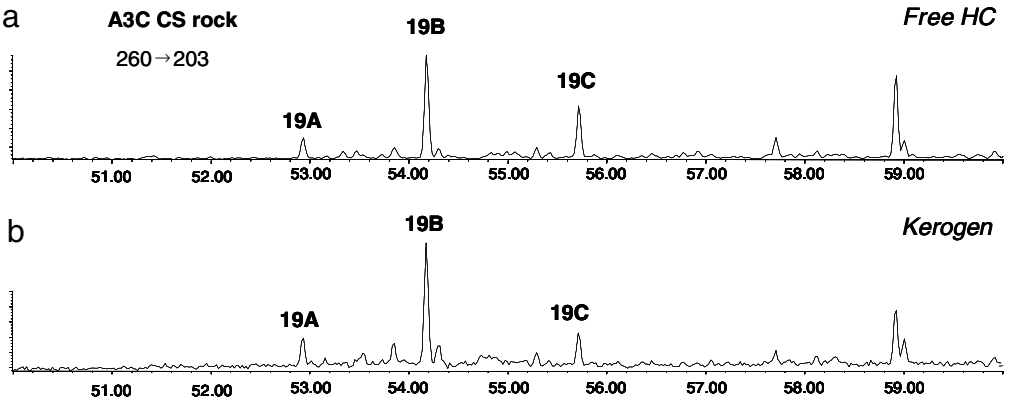

Fig. 9. MRM chromatograms 260 → 203 Da showing distributions of C_{19} A-norsteranes in (a) free alkane fraction and (b) kerogen-bound alkanes of a A3C CS rock.

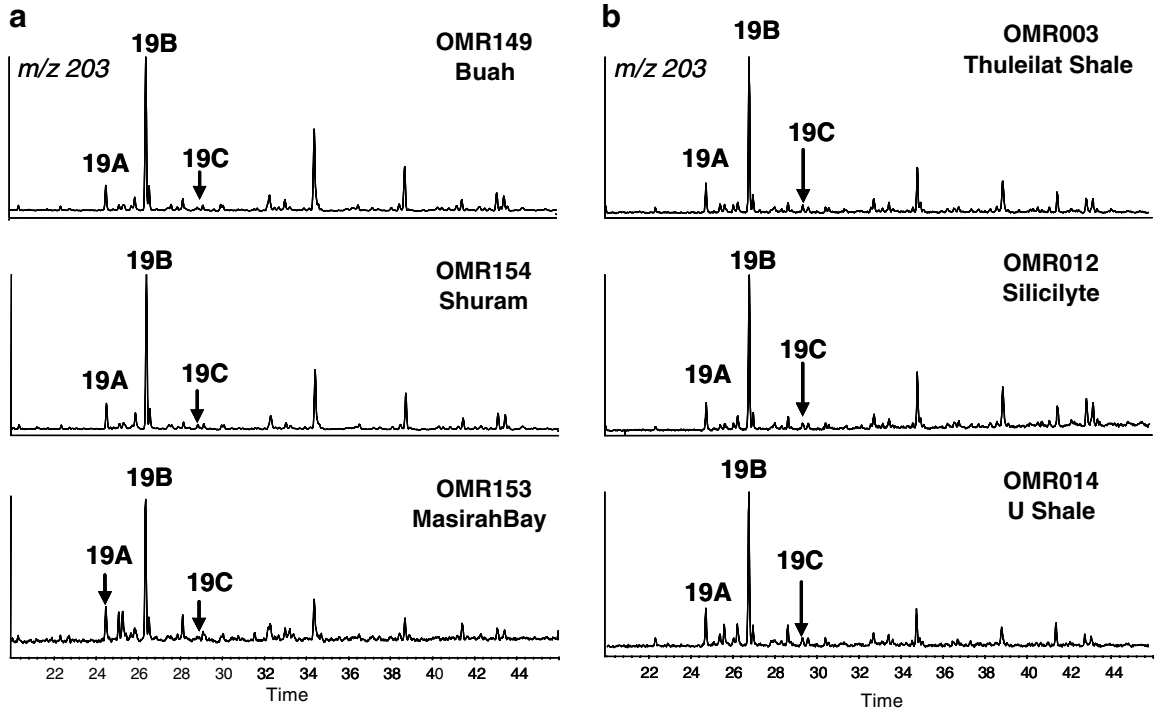

Fig. 10. Partial *m/z* 203 chromatograms showing distribution of C_{19} A-norsteranes in alkane fractions (a) of pre-salt rocks and (b) of Athel intra-salt rocks.

7. Oil geochemistry

Table 2 shows bulk properties for the oils as well as key biomarkers ratios obtained from MRM GC–MS. The fluid properties of the oils vary significantly. Silicilyte oils are all characterized by API gravity higher than 45°, whereas post-salt Huqf fluids tend to be quite heavy, with API between 3.4° and 29.1°. The API gravity of carbonate stringer oils is highly variable between 22.5° and 51.5°.

Bulk carbon isotopic data (Table 2) were obtained on the saturated and aromatic hydrocarbon fractions of the oils. Fig. 12a shows the familiar distinction of Q and Huqf oils based on the sterane carbon number distribution and carbon isotopic compositions. Within Huqf oils, bulk carbon isotopes of carbonate stringer oils span a wide range of values from −33‰ to −35.7‰. Silicilyte oils form a tighter group around −35‰. Post-salt Huqf oils are on average lighter than silicilyte and carbonate stringer oils, clustering around −36‰, with the exception of Jazal-1 at −34‰ (Table 2).

GC of the oil alkanes shows that more than half of the post-salt Huqf oils (10 of 15) and 2 of 6 Q oils are affected by biodegradation, evident through the loss of *n*-alkanes and acyclic isoprenoids and the presence of an unresolved complex mixture (Peters et al., 2005). The degree of biodegradation varies from moderate to severe [biodegradation ranks based on the Peters and Moldowan (1993) scale listed in Table 2]. Mild biodegradation is recognized by high Pr/C_{17} and Ph/C_{18} ratios, arising from the preferential bacterial degradation of *n*-alkanes (Connan, 1984). Post-salt Huqf oils Nimr OMO004 as well as Q oils Misfar and Ghufos are the most altered and show virtually complete removal of *n*-alkanes and isoprenoids. The relatively high proportion of C_{29} steranes (49%, Fig. 12a) and the very low abundance of C_{35} hopanes (Table 2) in Q oil Misfar result from the preferential degradation of C_{27} relative to higher C-number steranes and of C_{35} hopanes relative to lower C-number hopanes (Peters et al., 2005). Homologous series of 25-norhopanes were not detected even in the most severely biodegraded oils. Significantly, none of the carbonate stringer oils and

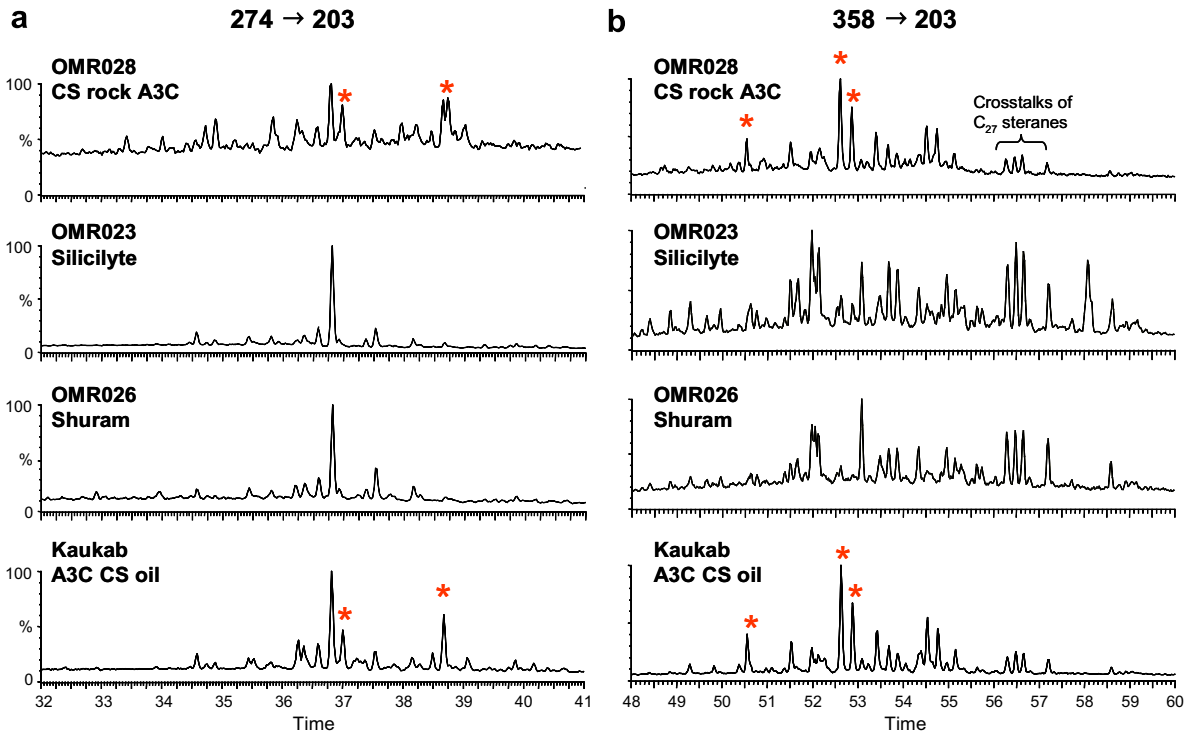

Fig. 11. MRM chromatograms for (a) 274 → 203 Da and (b) 358 → 203 Da showing distributions of C_{20} and C_{26} A-norsteranes, respectively, for rocks CS A3C OMR028, silicilyte OMR023, Shuram OMR026 and for CS oil Kaukab A3C.

silicilyte oils shows signs of biodegradation. Silicilyte hydrocarbons have condensate-like API gravity values and are all characterized by an extremely low biomarker content, challenging the acquisition of reliable sterane and hopanes measurement from conventional GC–MS. However, MRM GC-MS allows the detection limit to be reduced and enabled us to measure reproducible biomarker data for these oils.

Maturity-biomarker parameters such as 20S/(20S + 20R) and 20S αββ/(αββ + ααα) C_{29} steranes reach near end-point values (on average 0.53 and 0.59, respectively) indicating that SOSB oils have been generated at the peak stage of oil generation. Further differentiation of the oils' maturity is obtained from Ts/(Ts + Tm) and diasterane/sterane ratios (Fig. 12b). Silicilyte oils appear to be the most mature, with Ts/(Ts + Tm) values close to unity, consistent with their high API gravity. Q oils have also a relatively high maturity and post-salt Huqf oils and carbonate stringer oils are generally the least mature (early to peak oil window). However, carbonate stringer oils display a broad range of thermal maturity, which becomes even more apparent when their reservoir depths are evaluated (Fig. 13).

As previously found, Huqf oils consisting of post-salt oils, silicilyte and carbonate stringer oils have very similar patterns of biomarker hydrocarbons. The predominance of C_{29} steranes is pervasive, as are high concentrations of C_{35} hopanes, 28,30-dinorhopane and 25,28,30-trinorhopane (Fig. 12). This apparent similarity has obscured many of the more subtle features that might reflect more specific oil-source relationships. Distinct features displayed by Q oils in contrast to Huqf oils, include: much higher abundances of gammacerane, 28,30-dinorhopane (Fig. 12c) and 3-methylhopanes (Fig. 12d), as well as high C_{24}/C_{23} and low C_{22}/C_{21} cheilanthanes ratios (Fig. 12f).

The use of statistical analysis applied to biomarker data is essential to identify those geochemical parameters that best account for the variability in the entire data set and enable oil family relationships to be accurately and robustly established. PCA and HCA were applied to MRM GC–MS-derived biomarker ratios and used to delineate the oils into major families as well as to verify some of the distinctive characteristics of the rocks (data not shown). Biomarker ratios related to maturity were not considered for this exercise. PCA was used to identify 20 biomarker ratios that best account for the overall variability in the data. These were subsequently used to construct the cluster analysis in Fig. 14. Four compositional oil groupings can be distinguished and a map of resulting oil families is shown in Fig. 15:

(1) Family A consists of silicilyte oils exclusively.
(2) Family B is composed mainly of post-salt Huqf oils with two carbonate stringer oils (Dhahaban South A1C and Kaukab A1C). Within Family B, two sub-clusters appear.
(3) Family C is made up of carbonate stringer oils, with the exception of post-salt Huqf oil Ghufos and clusters into two major sub-groupings CI and CII, which are mainly geographically controlled. Indeed, CI is composed of carbonate stringer oils from the Birba field or geographically close, whereas CII consists primarily of carbonate stringer oils located in the southwestern part of the SOSB (Fig. 15). It appears that the pressure regime does not influence the groupings, as normally-pressured A2C oils Rabab/Sakhiya/Fayrouz/Zalzala cluster separately from normally-pressured A4C oils Budour and Birba North.
(4) Family D is comprised entirely of Q oils.

8. Oil-source rock correlations

8.1. Silicilyte oils

The silicilyte oils are very mature and so are characterized by API gravity above 45° and a very low biomarker content. Biomarker analysis with conventional GC–MS does not allow their detection

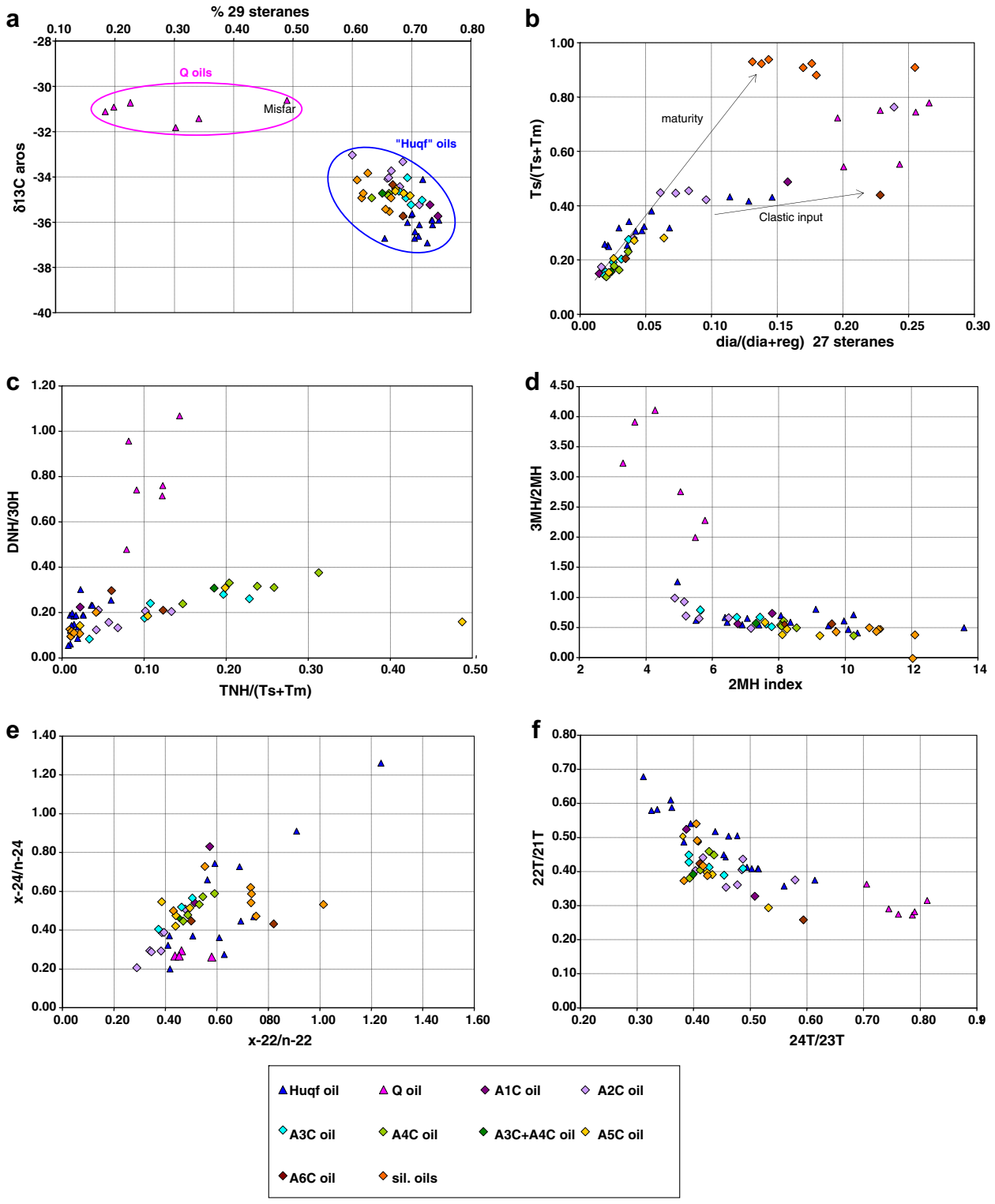

Fig. 12. Cross plots of selected biomarker parameters for SOSB oils. Refer to Table 2 for biomarker ratios. X-22: Mid-chain C_{22} MMAs; n-22: linear C_{22} alkane; dia/(dia + reg) 27 steranes = C_{27} diasteranes/(C_{27} regular steranes + C_{27} diasteranes).

and requires the sensitivity of a magnetic sector instrument using MRM for precise quantification. Most of the biomarker distributions in these oils reflect the high degree of maturity and are therefore of limited use for correlation purposes. Maturity has also affected bulk carbon isotopic values of silicilyte oils, shifting them towards heavier values and compromising their utility as a correlation tool.

However, clues about their origin are provided by a few maturity-independent parameters. The partial chromatogram generated from the MRM transition 260 → 203 Da reveals the lack of isomer 19C in the C_{19} A-norsteranes distributions of silicilyte oils, which rules out the carbonate stringers as a source (Fig. 16a). Several criteria indicate that silicilyte oils are mainly derived from Athel intra-salt rocks: they have high concentrations of mid-chain MMAs

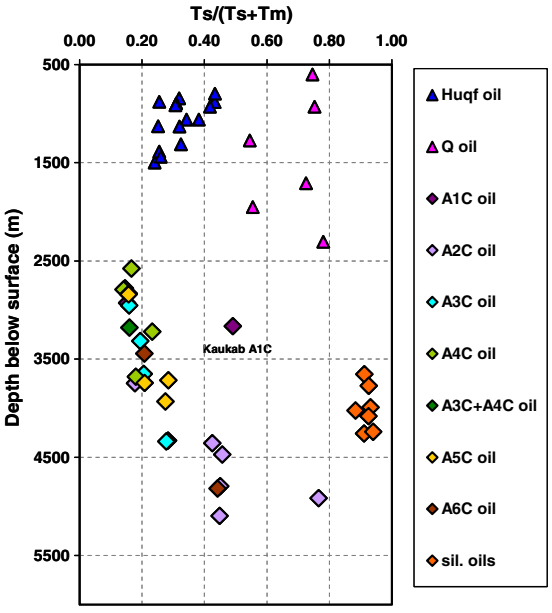

Fig. 13. Plot of Ts/(Ts + Tm) vs. reservoir depth for all SOSB oils.

(Fig. 12e), relatively high gammacerane contents (GA/30H = 0.21 on average) as well as a high proportion of C_{35} hopanes relative to C_{34} hopanes (Table 2). Additionally, silicilyte oils are among the SOSB oils showing the highest 2-methylhopane index values, which are associated with high 2-methylhopanes relative to 3-methylhopanes, as observed for Athel intra-salt rocks (3MeH/2MeH 0.4 on average for silicilyte oils and Athel intra-salt rocks; Fig. 12d).

The high relative abundance of 25,28,30-trinorhopane and 28,30-dinorhopane, characteristic of the Athel intra-salt rocks, is not a feature of silicilyte oils due to their elevated maturity (Fig. 12c). Athel intra-salt rocks are in contrast immature, as shown by T_{max} values (Table 1) and triaromatic steroid index values (data not shown). This discrepancy in thermal history reflects sample availability within the silicilyte oils since virtually all are found in deep reservoirs (between 3500 and 4000 m). In contrast, the maximum depth for the Athel intra-salt rocks analyzed is 2300 m. The ratio of 28,30-dinorhopane to 25,28,30-trinorhopane (DNH/TNH) is useful for circumventing the problem of maturity differences between rocks and oils, since it remains unaffected during maturation (Peters et al., 2005). Silicilyte oils have on average a DNH/TNH value of 2.3, a close match with the average exhibited by Athel intra-salt rocks (Table 3), providing additional evidence for their correlation.

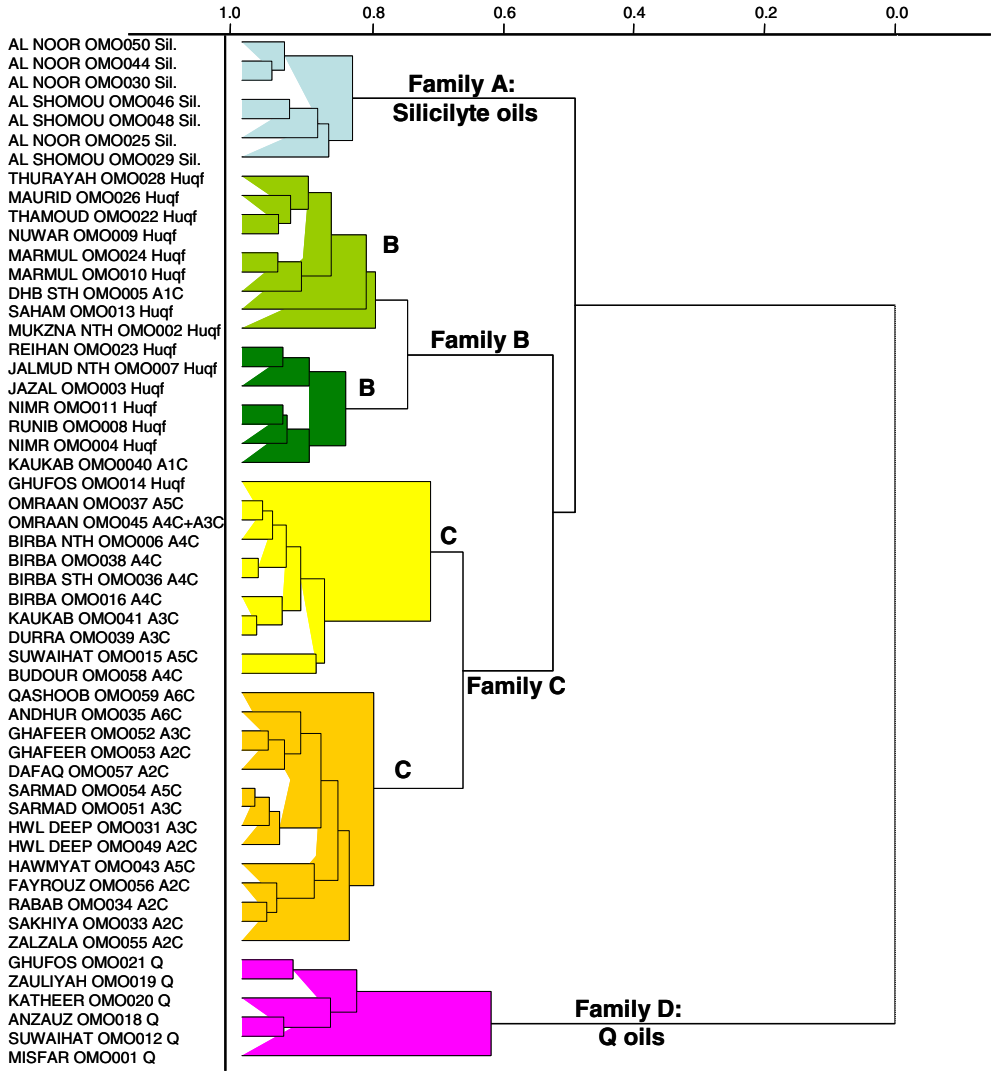

Fig. 14. Cluster analysis dendogram showing principal oil families in the SOSB.

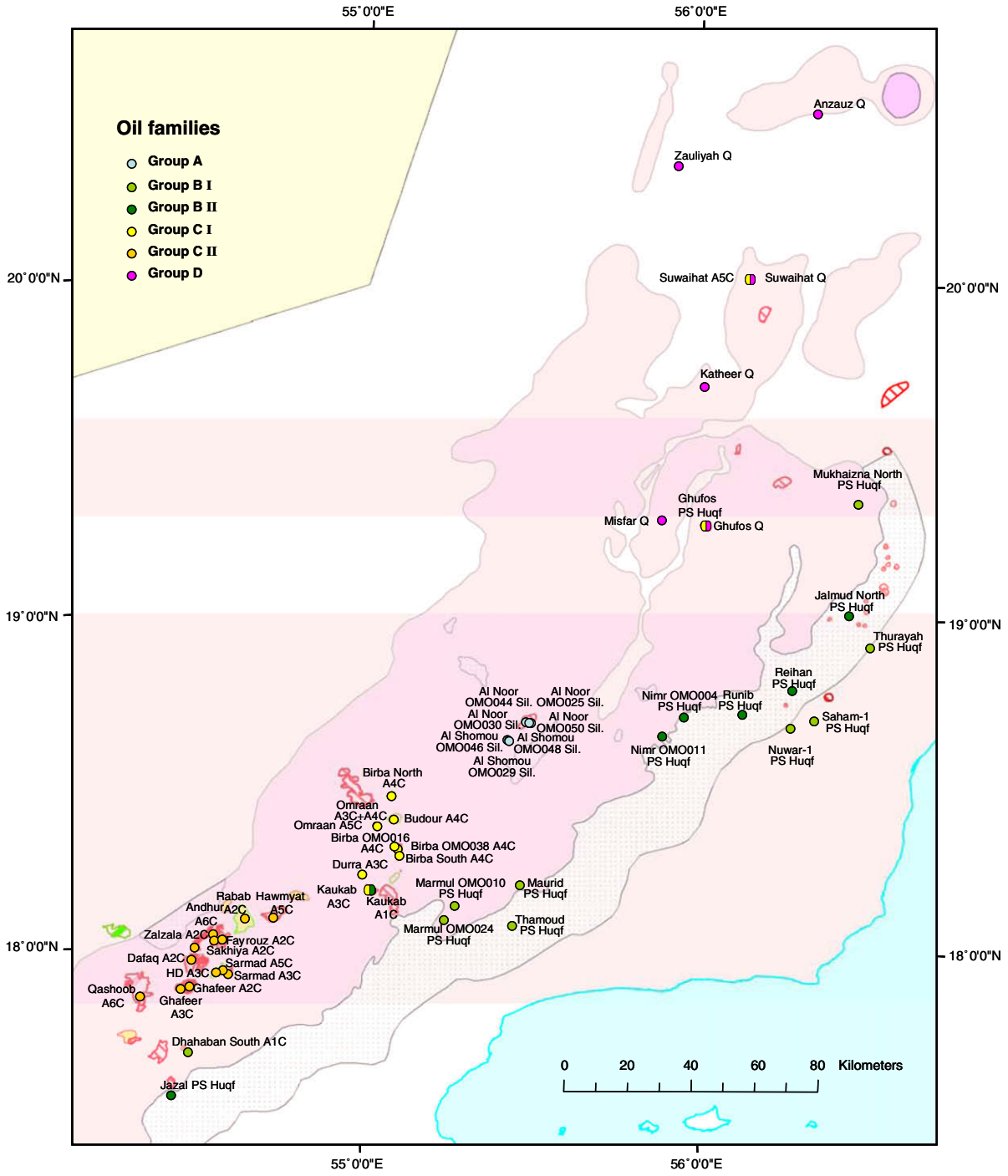

Fig. 15. Location map of oils coded by family as identified by hierarchical cluster analysis of biomarker compositions.

Further discrimination between Athel intra-salt rocks samples has proven difficult. However, we note that among other close similarities, mid-chain MMAs are especially abundant in the Athel Silicilyte and Thuleilat Fm samples, in comparison with the U Shale.

8.2. Carbonate stringer play

The origin of the charge for carbonate stringer accumulations is highly conjectural and two main mechanisms have been proposed. A first charging model involves the contribution of source rocks from the Nafun Group which, by all standards, are of exceedingly high quality. However, this scenario is challenged by the fact that the stringers are (or were previously), fully encased in salt, with no tangible access to regional oil charge, with the exception of some of the lower stringer units which, from drilling results, grounded on Nafun rocks. An example of this is the Kaukab A1C accumulation. Isolation of stringers in the salt has, in fact, led geologists to favour a self-charging mechanism with the carbonate stringers acting both as source rock and reservoir. Yet, the apparent lack of source rock potential, based on low TOC relative to other units in the carbonate stringers, as well as the absence of unequivocal geochemical evidence supporting this hypothesis has up to now undermined the self-sourcing scenario.

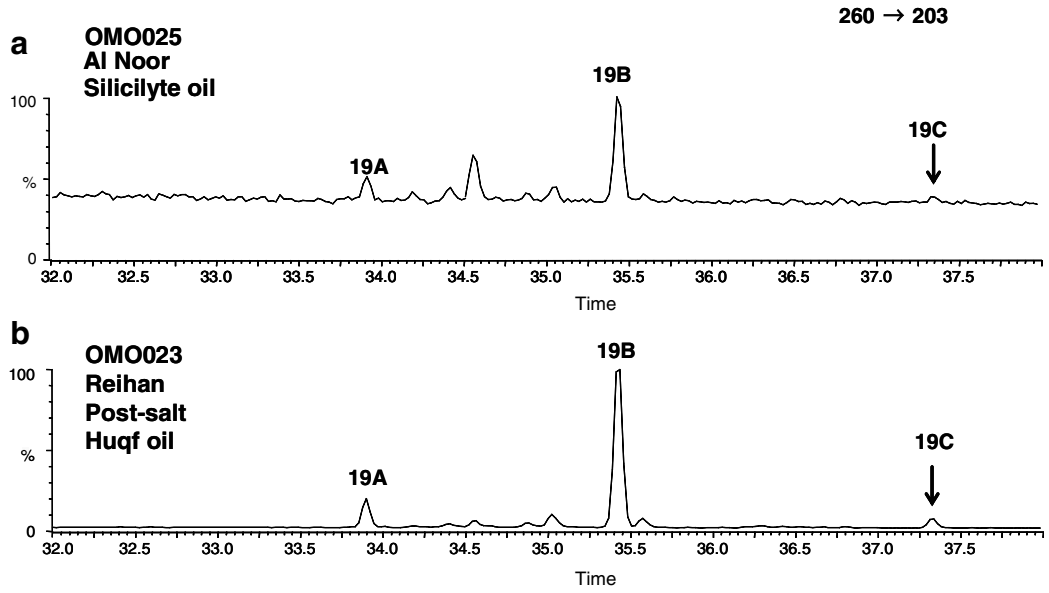

Fig. 16. MRM chromatograms 260 → 203 Da showing distributions of C_{19} A-norsteranes in alkane fractions of (a) Al Noor silicilyte oil (OMO025) and (b) Reihan post-salt Huqf oil.

The putative A-norsteranes, described in section 6.4, shed light on the source of the carbonate stringer oils. The C_{19} A-norsterane pattern, with the 19C isomer in significant abundance along with isomers 19A and 19B, observed in carbonate stringer rocks, is present in virtually all produced carbonate stringer oils from each stratigraphic interval (Fig. 17). The 19C/19A and 19B/19A ratios enable a clear distinction between the carbonate stringer rocks and oils and Nafun rocks/Athel intra-salt rocks, as illustrated in Fig. 18. Furthermore, the C_{20} and C_{26} A-norsterane distributions in the carbonate stringer oils mimic those of the carbonate stringer bitumens, and contain A-norsterane isomers that are missing from pre-salt and Athel intra-salt rocks (Fig. 11). This efficient discrimination of carbonate stringer rocks and oils from pre-salt and Athel intra-salt rocks through A-norsterane distributions provides strong and novel evidence that the carbonate stringer oils are predominantly self-sourced. Indeed, the fact that concentrations of isomers 19A and 19B are of the same order of magnitude in carbonate stringers and Nafun rocks indicates that any significant input of C_{12} + hydrocarbons from the latter in carbonate stringer oil accumulations should be evident through dilution of compound 19C compared to 19A and 19B, which is rarely the case.

Additional lines of evidence adding weight to the proposal that carbonate stringer oils are self-sourced can be summarized as follows:

- The trend of increasing thermal maturity with depth displayed by the Ts/Tm ratio plotted against reservoir depth in the carbonate stringers (Fig. 13) provides additional indirect confirmation of local sourcing for the majority of these accumulations, as opposed to migration from deeper rocks.
- Statistical cluster analysis based on biomarker ratios, which did not include the discriminating A-norsteranes 19C/19A ratio, clearly showed that the bulk of the carbonate stringer oils cluster separately from the other oils in the SOSB as a distinct oil grouping (Fig. 14).
- Biomarker distributions within free and kerogen-bound aliphatic fractions of carbonate stringer rocks show strong similarities to those of carbonate stringer oils. Details will be reported elsewhere (Stalvies et al., unpublished results).

8.3. Mixed accumulations in the carbonate stringers

Carbonate stringer oils with low relative abundance of isomers 19C (Kaukab A1C, Suwaihat A5C, Qashoob A6C and Dhahaban South A1C, inset Fig. 18) might be interpreted as partially produced from Nafun rocks, since mixing of a carbonate stringer charge and a pre-salt charge would lead to a dilution of C_{19} A-norsterane 19C relative to isomers 19A and 19B in the resulting accumulation. Of these oils, Kaukab A1C and Dhahaban South A1C did not fall into the main carbonate stringer family C in the hierarchical cluster analysis dendrogram (Fig. 14) and are found in reservoirs with potential access to Nafun sediments. Within carbonate stringer sub-cluster CII, Qashoob stands out as an outlier (Fig. 14). Such statistical outliers can result from the mixing of sources representing different end members or unrecognized source rocks. A mixed character for these crudes is evident from examination of their biomarker ratios, which reveals discrepancies from the average values presented by carbonate stringer oils. Kaukab A1C, Dhahaban South A1C, Suwaihat A5C and Qashoob A6C share characteristics with Nafun rocks while exhibiting typical carbonate stringer oil features as illustrated in Table 4. Kaukab A1C is also one of the oils with a thermal maturity off the trend observed for carbonate stringer oils (Fig. 13). The thermal maturity of Kaukab A1C as revealed by Ts/(Ts + Tm) appears to be higher than predicted from its reservoir depth, suggesting a pre-salt contribution for this oil rather than entirely local sourcing. Compound-specific hydrogen isotopic data confirm this (data not shown).

Deciphering the input from pre-salt rocks in the carbonate stringer oils via the lack of a specific marker for the pre-salt section is not trivial. The possibility that these apparently conflicting ratios may result from local variations in the composition of the carbonate stringers producing these outliers cannot be ruled out at this stage.

8.4. Post-salt Huqf oils

Of the post-salt Huqf oils analyzed, few show the 19C norsterane isomer, precluding significant charge from carbonate stringers to the Phanerozoic reservoirs (Figs. 16b and 19). One notable

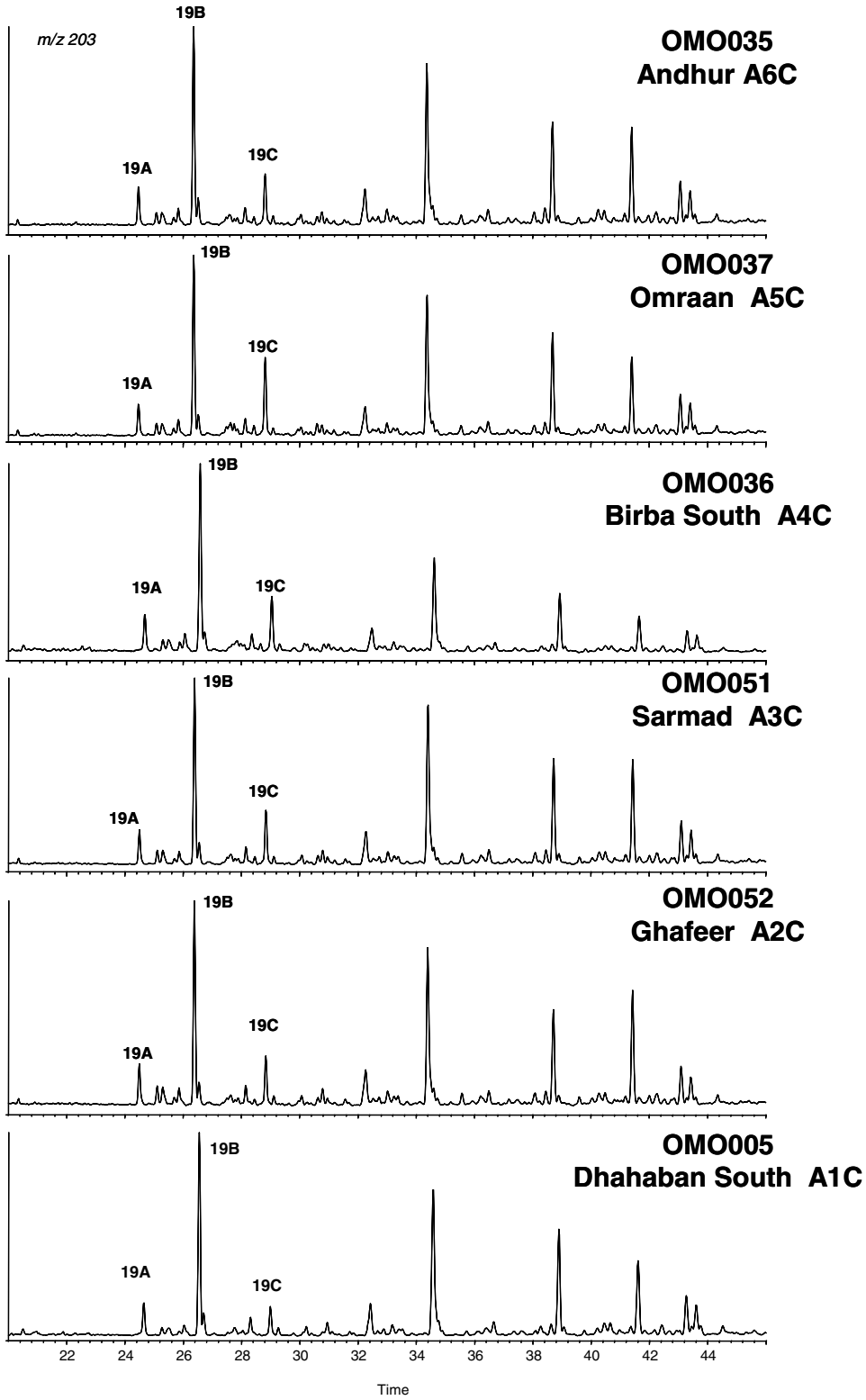

Fig. 17. Partial *m/z* 203 chromatograms showing distribution of C_{19} A-norsteranes in alkane fractions of carbonate stringer oils.

exception is the Jazal sample, which also shows relatively heavy $\delta^{13}C$ values (−33.9‰ for saturates and −34.1‰ for aromatics) when compared with the rest of post-salt Huqf oils. The relatively abundant 19C A-norsterane, along with carbon isotopic compositions similar to those of carbonate stringer oils suggest that the Jazal accumulation has a strong carbonate stringer input.

The challenge for understanding Eastern Flank reservoir charge is in reliably assessing the contribution of Nafun rocks and Athel Basin intra-salt rocks, respectively. Difficulties arise from the lack of specific biomarkers for the pre-salt section, which could contribute subtly to any oil, and from the variability in the biomarker character within given Nafun formations (cf. Section 6.3). Average

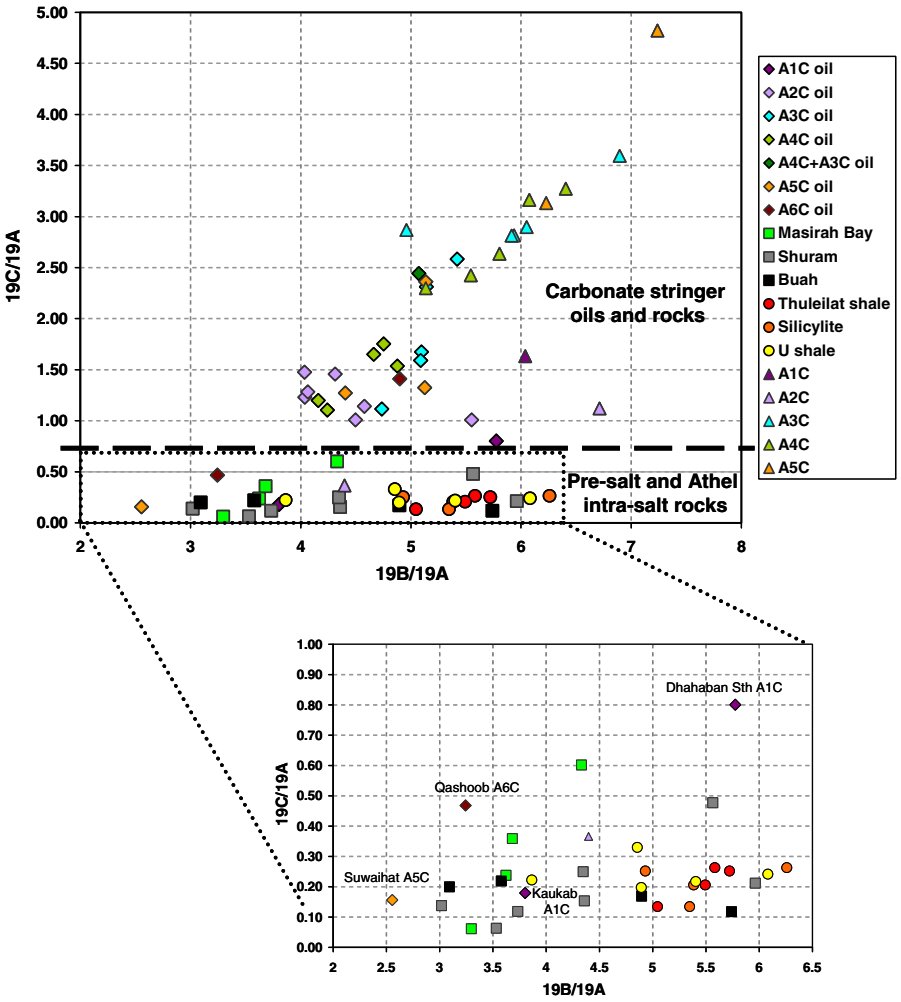

Fig. 18. Plot of 19C/19A vs. 19B/19A for all Huqf rocks and carbonate stringer oils.

Table 4
Summary of biomarker characteristics exhibited by selected post-salt Huqf and carbonate stringer oils (Refer to Table 2 for ratios; MMAs: mid-chain monomethyl alkanes)

Oil	Stratigraphy	Pre-salt characteristics	Intra-salt characteristics
Nuwar	PS Huqf		High GA/30H, high 22T/21T, low 23T/24T, high 2MHI
Maurid	PS Huqf		High GA/30H, high 22T/21T, low 23T/24T, high 2MHI, high DNH/30H
Mukhaizna North	PS Huqf		High 35H/34H, high 22T/21T, low 23T/24T
Ghufos	PS Huqf		High 35H/34H, high 22T/21T, low 23T/24T, high 2MHI
Runib	PS Huqf	Low GA/30H, low 35H/34H Low 22T/21T, high 23T/24T Low 2MHI	
Nimr	PS Huqf	Low GA/30H, low 35H/34H Low 22T/21T, high 23T/24T	
Kaukab	A1C	Low 35H/34H, low GA/30H Low DNH/30H, low TNH/(Ts + Tm), low 22T/21T, high 23T/24T	High 2MHI, high MMAs
Dhahaban	A1C	Low TNH/(Ts + Tm), low GA/30H	High 22T/21T, low 23T/24T
Suwaihat	A5C	Low GA/30H, low TNH/(Ts + Tm)	High 2MHI, high 2MH/3MH High 22T/21T, low 23T/24T
Qashoob	A6C	Low 35H/34H, low 22T/21T, high 23T/24T	High 2MHI, high DNH/30H

trends for the potentially opposing Athel intra-salt and Nafun rocks summarized in Table 3 are used here to detect respective inputs. Briefly, the most useful parameters were relative abundance of C_{35} hopanes, gammacerane, MMAs, 28,30-dinorhopane and 25,28,30-trinorhopane, proportion of 2α-methylhopanes relative to 3β-methylhopanes, 2-methylhopane index, and 22T/21T and 24T/23T ratios.

Post-salt Huqf oils have on average high relative abundances of gammacerane and high 35H/34H values at levels comparable only with those observed for Thuleilat Fm. and Athel Silicilyte samples (Table 2). This alone indicates that the latter contribute predominantly to accumulations in the Phanerozoic reservoirs of the Eastern Flank. Bulk carbon isotopic compositions also tend to support a main Athel intra-salt charge for the post-salt Huqf oils: the latter are characterized by ^{13}C-depleted saturated and aromatic hydrocarbon fractions in comparison with other SOSB oils (Fig. 12a, Table 2), in spite of the fact that most of these oils are affected by biodegradation, which is known to shift $\delta^{13}C$ towards heavier values. With the exception of Jazal, bulk $\delta^{13}C$ values of saturated hydrocarbon fractions in post-salt Huqf oils form a very tight cluster from

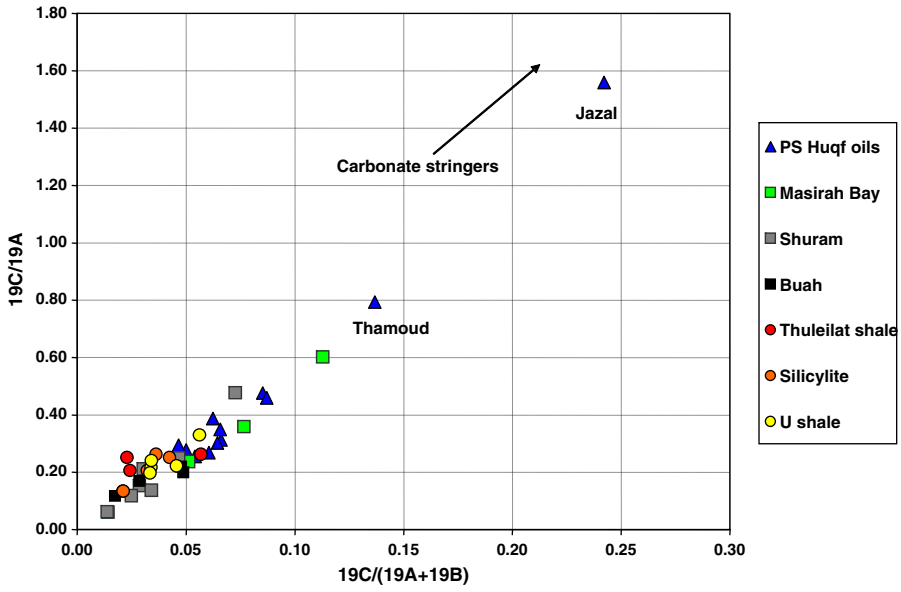

Fig. 19. Plot of 19C/19A vs. 19B/19A for Huqf rocks and post-salt Huqf oils.

−34.8‰ to −36.2‰, which corresponds best to the range of values exhibited by Thuleilat Fm. and Athel Silicilyte rocks, even more so if the effects of biodegradation are considered.

However, the degree to which these formations contribute to Eastern Flank reservoirs is variable. Some post-salt Huqf oils including Mukhaizna North, Nuwar, Ghufos and Maurid show a strong Athel intra-salt character as suggested from a combination of biomarker ratios (Table 4). Ghufos is the only post-salt Huqf oil clustering with carbonate stringer oils. However, the low relative abundance of 19C A-norsterane in this oil rules out charging from carbonate stringers. The clustering of post-salt Huqf Ghufos with carbonate stringer oils reflects its affinity with the Ara character. In contrast, Runib, Nimr OMO004 and Nimr OMO011 appear to have a Nafun affinity. The difference in biomarker character of these two sets of post-salt Huqf oils is revealed in the cluster analysis dendrogram (Fig. 14) where Mukhaizna North, Nuwar and Maurid cluster as a separate sub-grouping (Family BI) from Runib, Nimr OMO004 and Nimr OMO011 oils (Family BII) (Fig. 14). Runib, Nimr OMO004 and Nimr OMO011 oils cluster with Kaukab A1C, which also showed strong pre-salt affinities. It is therefore feasible, but not proven, that the oils clustering as family BII have some component of Nafun hydrocarbons.

The apparent absence of abundant hydrocarbon deposits or even residual oil derived from Nafun rocks, which are by any measure very good source rocks, is perplexing. Previous workers have suggested (Paul Taylor, personal communication) that there was a potential disjunction between hydrocarbon generation and emplacement of traps or seals. The demonstration herein that virtually all the SOSB hydrocarbons originate from within the Ara (i.e. intra-salt) sequence, either in carbonate stringers or within the Athel sub-basin, offers verification of this. Oil generation from OM within the salt sequence will be slower and occur later than for the Nafun rocks due to the insulating properties of the evaporite minerals. The carbonate mineral matrix of most Ara sediments also helps suppress catagenesis over long geological times (> 540 Ma), compared to clastic source rocks which would have generated lighter oil and more gas. Moreover, apart from the lower stringers, many intra-salt reservoirs are subject to significant overpressure, further retarding catagenesis. Hydrocarbons generated and reservoired within the salt could, therefore, be retained until geologically more recent times, while those generated outside would have been lost. Apparently, relatively recent salt movement has allowed some leakage from the Athel sub-basin, accounting for the oils now found in the Phanerozoic Eastern Flank reservoirs.

9. Conclusions

A new geochemical basis has been established for oil source correlation in the South Oman Salt Basin. Novel steroidal biomarkers, as well as the more commonly used steroids and triterpenoids show secular and palaeoenvironmental changes through the Nafun and Ara Groups of the Huqf Supergroup, which helped establish reliable oil-source correlations.

The source rocks that are positively identified as contributing to significant hydrocarbon accumulations comprise the Ara carbonate stringers and the Athel sub-basin sediments (U, Thuleilat and Athel Silicilyte). The relative abundances of novel compounds interpreted as being A-norsteranes were found to be invaluable for distinguishing carbonate stringer bitumens, kerogens and their derived oils from other kinds of SOSB hydrocarbons. The patterns of C_{19} A-norsteranes suggest that the bulk of the carbonate stringer oils are self sourced. This key finding is supported by additional independent geochemical data including, especially, the ranking of maturity derived from C_{27} hopanoids and present day burial depth. The C_{19} A-norsteranes are accompanied by C_{20} counterparts and probable precursors with intact side chains, readily detected by $M^+ \rightarrow 203$ Da fragmentation reactions in GC–MS–MS.

Deciphering and quantifying inputs from Nafun rocks to oil accumulations has proved challenging, with the lack of specific markers for the pre-salt section. The most useful geochemical characteristics delineating Nafun Group organic matter from Ara Group intra-salt source rocks include: low relative abundance of mid-chain monomethylalkanes (X-compounds); low relative abundance of gammacerane, 28,30-dinorhopane, 25,28,30-trinorhopane and 2-methylhopanes; low $C_{22}T/C_{21}T$ and high $C_{23}T/C_{24}T$ cheilanthane ratios. Based on these parameters, Ara source rocks were found to be the predominant source for Huqf oils. Subtle aspects of the composition of some carbonate stringer and post-salt Huqf oils could suggest some degree of sourcing from the Nafun rocks but stronger evidence is needed to confirm this.

Acknowledgments

J. Grotzinger (Caltech) and S. Bowring (MIT) contributed significantly to the formulation of this study. P. Taylor, M. Newall, Z. Rawahi, S. Ochs, J. Schreurs and H. Al-Siyabi (Petroleum Development Oman) and S. Schröder (MIT) contributed numerous valuable ideas and suggestions, especially in respect of the local geology and geochemistry. A. Lewis, L. Bradtmiller, Y. Hebting, R. Kayser, C. Colonero and S. Lincoln contributed to various stages of the work at MIT. P. Farrimond first identified the anomalous abundances of C_{19} steroidal hydrocarbons in some SOSB oils and alerted us to their potential value as tools for correlation. Some Rock-Eval data and bitumen isolation were carried out at Geoscience Australia by R. Davenport. Petroleum and cuttings composites, accompanied by bulk geochemical data, were provided by Shell International E&P. Petroleum Development of Oman provided financial support for the work. R.E.S. and G.D.L. gratefully acknowledge further support by way of grants from the NASA Exobiology Program and NSF Biocomplexity Program. We thank the Ministry of Oil and Gas of the Sultanate of Oman for permission to publish. Finally, the manuscript greatly benefited from constructive comments by Hans Nytoft and Ger Van Graas.

Appendix A. Supplementary data

Supplementary data associated with this article can be found, in the online version, at doi:10.1016/j.orggeochem.2008.09.011.

Associate Editor—**C.C. Walters**

References

Allen, P.A., Leather, J., 2006. Post-Marinoan marine siliciclastic sedimentation: the Masirah Bay Formation, Neoproterozoic Huqf Supergroup of Oman. Precambrian Research 144, 167–198.

Al-Marjeby, A., Nash, D.F., 1986. A summary of the geology and oil habitat of the Eastern Flank hydrocarbon province of South Oman. Marine and Petroleum Geology 3, 306–314.

Al-Siyabi, H.A., 2005. Exploration history of the Ara intrasalt carbonate stringers in the South Oman Salt Basin. GeoArabia 10, 39–72.

Amthor, J.E., Faulkner, T., Frewin, N.L., Alixant, J.-L., Matter, A., Ramseyer, K., 1998. The Athel play in Oman: controls on reservoir quality (Abstract). GeoArabia 3, 62.

Amthor, J.E., Grotzinger, J.P., Schröder, S., Bowring, S.A., Ramezani, J., Martin, M.W., Matter, A., 2003. Extinction of *Cloudina* and *Namacalathus* at the Precambrian–Cambrian boundary in Oman. Geology 31, 431–434.

Amthor, J.E., Ramseyer, K., Faulkner, T., Lucas, P., 2005. Stratigraphy and sedimentology of a chert reservoir at the Precambrian–Cambrian Boundary: the Al Shomou Silicilyte, South Oman Salt Basin. GeoArabia 10, 89–122.

Andrusevich, V.E., Engel, M.H., Zumberge, J.E., Brothers, L.A., 1998. Secular, episodic changes in stable carbon isotope composition of crude oils. Chemical Geology 152, 59–72.

Bazhenova, O.K., Arefiev, O.A., 1997. Geochemical peculiarities of Pre-Cambrian source rocks in the East European Platform. Organic Geochemistry 25, 341–351.

Bohlin, L., Gehrken, H.P., Scheuer, P.J., Djerassi, C., 1980. Minor and trace sterols in marine invertebrates. XVI: 3β-Hydroxymethyl-A-nor-5α-gorgostane, a novel sponge sterol. Steroids 35, 295–304.

Bohlin, L., Sjöstrand, U., Djerassi, C., Sullivan, B.W., 1981. Minor and trace sterols in marine invertebrates: 20. 3-β-hydroxymethyl-A-norpatinosterol and 3-β-hydroxymethyl-A-nordinosterol: two new sterols with modified nucleus and side chain from the sponge, *Teichaxinella morchella*. Journal of the Chemical Society, Perkin Transactions 1, 1023–1028.

Bowring, S.A., Grotzinger, J.P., Condon, D.J., Ramezani, J., Newall, M., 2007. Geochronologic constraints on the chronostratigraphic framework of the Neoproterozoic Huqf Supergroup, Sultanate of Oman. American Journal of Science 307, 1097–1145.

Brasier, M., McCarron, G., Tucker, R., Leather, J., Allen, P., Shields, G., 2000. New U–Pb zircon dates for the Neoproterozoic Ghubrah glaciation and for the top of the Huqf Supergroup, Oman. Geology 28, 175–178.

Brincat, D., Abbott, G.D., 2001. Some aspects of the molecular biogeochemistry of laminated and massive rocks from the Naples Beach Section (Santa Barbara-Ventura Basin). In: Isaacs, C.M., Rullkötter, J. (Eds.), The Monterey Formation: From Rocks to Molecules. Columbia University Press, New York, pp. 140–149.

Brocks, J.J., Summons, R.E., 2003. Sedimentary hydrocarbons, biomarkers for early life. In: Holland, H.D., Turekian, K.K. (Eds.), Treatise on Geochemistry. Pergamon, Oxford, pp. 63–115.

Condon, D.J., Zhu, M., Bowring, S.A., Wang, W., Yang, A., Jin, Y., 2005. U–Pb Ages from the Neoproterozoic Doushantuo Formation, China. Science 308, 95–98.

Connan, J., 1984. Biodegradation of crude oils in reservoirs. In: Brooks, J., Welte, D.H. (Eds.), Advances in Petroleum Geochemistry, vol. 1. Academic Press, New York, pp. 299–335.

Cozzi, A., Al-Siyabi, H.A., 2004. Sedimentology and play potential of the late Neoproterozoic Buah Carbonates of Oman. GeoArabia 9, 11–36.

Cozzi, A., Allen, P.A., Grotzinger, J.P., 2004. Understanding carbonate ramp dynamics using δ^{13} C profiles: examples from the Neoproterozoic Buah Formation of Oman. Terra Nova 16, 62–67.

Curiale, J.A., Cameron, D., Davis, D.V., 1985. Biological marker distribution and significance in oils and rocks of the Monterey Formation, California. Geochimica et Cosmochimica Acta 49, 271–288.

de Leeuw, J.W., Sinninghe Damsté, J.S., Schenck, P.A., Boon, J.J., 1985. Biogeochemistry of Gavish Sabkha sediments. I: Studies on neutral reducing sugars and lipid moieties by gas chromatography–mass spectrometry. In: Friedman, G.M., Krumbein, W.E. (Eds.), Hypersaline Ecosystems The Gavish Sabkha. Springer, Heidelberg, pp. 350–367.

Espitalié, J., Deroo, G., Marquis, F., 1985. La pyrolyse Rock-Eval et ses applications. Revue de l'Institut Français du Pétrole 40, 563–579 (755–784).

Fike, D.A., Grotzinger, J.P., Pratt, L.M., Summons, R.E., 2006. Oxidation of the Ediacaran Ocean. Nature 444, 744–747.

Fowler, M.G., Douglas, A.G., 1987. Saturated hydrocarbon biomarkers in oils of Late Precambrian age from eastern Siberia. Organic Geochemistry 11, 201–213.

Gelin, F., Frewin, N., Huc, A.-Y., Kowalewski, I., Amthor, J.E., 1999. Depositional model for Infracambrian organic matter in South Oman Basin (Abstract). In: 19th International Meeting on Organic Geochemistry Abstracts, Part I, Istanbul, pp. 389–390.

Gelpi, E., Schneider, H., Mann, J., Oró, J., 1970. Hydrocarbons of geochemical significance in microscopic algae. Phytochemistry 9, 603–612.

Gorin, G.E., Racz, L.G., Walter, M.R., 1982. Late Precambrian–Cambrian sediments of Huqf group, Sultanate of Oman. American Association of Petroleum Geologists Bulletin 66, 2609–2627.

Grantham, P.J., 1986. The occurrence of unusual C_{27} and C_{29} sterane predominances in two types of Oman crude oil. Organic Geochemistry 9, 1–10.

Grantham, P.J., Lijmbach, G.W.M., Posthuma, J., Hughes Clarke, M.W., Willink, R.J., 1987. Origin of crude oils in Oman. Journal of Petroleum Geology 11, 61–80.

Grantham, P.J., Wakefield, L.L., 1988. Variations in the sterane carbon number distributions of marine source rock derived crude oils through geological time. Organic Geochemistry 12, 61–73.

Grotzinger, J., Al-Siyabi, H., Al-Hashmi, R., Cozzi, A., 2002. New model for tectonic evolution of Neoproterozoic–Cambrian Huqf supergroup basins, Oman. GeoArabia 7, 241.

Guzmán-Vega, M.A., Moldowan, J.M., Fago, F.J., 1997. Upper Jurassic organic-rich depositional environments in the Tampico-Misantla Basin, Eastern Mexico (Abstract). In: 18th International Meeting on Organic Geochemistry Abstracts, Maastricht, pp. 157–158.

Halverson, G.P., Hoffman, P.F., Schrag, D.P., Kaufman, A.J., 2002. A major perturbation of the carbon cycle before the Ghaub glaciation (Neoproterozoic) in Namibia: prelude to snowball Earth? Geochemistry, Geophysics, Geosystems 3, doi: 10.1029/2001GC000244.

Halverson, G.P., Hoffman, P.F., Schrag, D.P., Maloof, A.C., Rice, A.H.N., 2005. Toward a Neoproterozoic composite carbon-isotope record. Geological Society of America Bulletin 117, 1181–1207.

Höld, I.M., Schouten, S., Jellema, J., Sinninghe Damsté, J.S., 1999. Origin of free and bound mid-chain methyl alkanes in oils, bitumens and kerogens of the marine, Infracambrian Huqf Formation (Oman). Organic Geochemistry 30, 1411–1428.

Konert, G., Visser, W., van den Brink, H., 1991. Generation, migration and entrapment of Precambrian oils in the eastern flank Hevay Oil province, South Oman (abstract). American Association of Petroleum Geologists Bulletin 75, 1413.

Le Guerroué, E., Allen, P.A., Cozzi, A., 2006a. Chemostratigraphic and sedimentological framework of the largest negative carbon isotopic excursion in Earth history: the Neoproterozoic Shuram Formation (Nafun Group, Oman). Precambrian Research 146, 68–92.

Le Guerroué, E., Allen, P.A., Cozzi, A., Etienne, J.L., Fanning, M., 2006b. 50 Myr recovery from the largest negative δ^{13}C excursion in the Ediacaran ocean. Terra Nova 18, 147–153.

Loosveld, R., Bell, A., Terken, J., 1996. The tectonic evolution of interior of Oman. GeoArabia 1, 28–51.

Love, G.D., McAulay, A., Snape, C.E., Bishop, A.N., 1997. Effect of process variables in catalytic hydropyrolysis on the release of covalently bound aliphatic hydrocarbons from sedimentary organic matter. Energy and Fuels 11, 522–531.

Mattes, B.W., Conway Morris, S., 1990. Carbonate/evaporite deposition in the Late Precambrian–Early Cambrian Ara Formation of Southern Oman. In: Robertson, A.H.F., Searle, M.P., Ries, A.C. (Eds.), The Geology and Tectonics of the Oman Region, vol. 49. Geological Society Special Publication, pp. 617–636.

McCaffrey, M.A., Moldowan, J.M., Lipton, P.A., Summons, R.E., Peters, K.E., Jeganathan, A., Watt, D.S., 1994. Paleoenvironmental implications of novel C_{30} steranes in Precambrian to Cenozoic age petroleum and bitumen. Geochimica et Cosmochimica Acta 58, 529–532.

McKirdy, D.M., Webster, L.J., Arouri, K.R., Grey, K., Gostin, V.A., 2006. Contrasting sterane signatures in Neoproterozoic marine rocks of Australia before and after the Acraman asteroid impact. Organic Geochemistry 37, 189–207.

Mello, M.R., Telnaes, N., Gaglianone, P.C., Chicarelli, M.I., Brassell, S.C., Maxwell, J.R., 1988. Organic geochemical characterization of depositional

palaeoenvironments of source rocks and oils in Brazilian marginal basins. Organic Geochemistry 13, 31–45.
Minale, L., Sodano, G., 1974. Unique 3β-hydroxymethyl-A-5α-steranes from the sponge *Axinella verrucosa*. Journal of the Chemical Society Perkin Transactions 1, 2380–2384.
Moldowan, J.M., Fago, F.J., Lee, C.Y., Jacobson, S.R., Watt, D.S., Slougui, N.-E., Jeganathan, A., Young, D.C., 1990. Sedimentary 24–*n*-propylcholestanes, molecular fossils diagnostic of marine algae. Science 247, 309–312.
Moldowan, J.M., Lee, C.Y., Watt, D.S., Jeganathan, A., Slougui, N.-E., Gallegos, E.J., 1991. Analysis and occurrence of C_{26} steranes in petroleum and source rocks. Geochimica et Cosmochimica Acta 55, 1065–1081.
Moldowan, J.M., Seifert, W.K., 1984. Structure proof and significance of stereoisomeric 28,30-bisnorhopanes in petroleum and petroleum source rocks. Geochimica et Cosmochimica Acta 48, 1651–1661.
Moldowan, J.M., Seifert, W.K., Gallegos, E.J., 1985. Relationship between petroleum composition and depositional environment of petroleum source rocks. American Association of Petroleum Geologists Bulletin 69, 1255–1268.
Noble, R., Alexander, R., Kagi, R.I., 1985. The occurrence of bisnorhopane, trisnorhopane and 25-norhopanes as free hydrocarbons in some Australian shales. Organic Geochemistry 8, 171–176.
Paoletti, C., Pushparaj, B., Florenzano, G., Capella, P., Lercker, G., 1976. Unsaponifiable matter of green and blue-green algal lipids as a factor of biochemical differentiation of their biomasses. I: Total unsaponifiable and hydrocarbon fraction. Lipids 11, 258–265.
Peters, K.E., Clark, M.E., das Gupta, U., McCaffrey, M.A., Lee, C.Y., 1995. Recognition of an Infracambrian source rock based on biomarkers in the Baghewala-1 oil, India. American Association of Petroleum Geologists Bulletin 79, 1481–1494.
Peters, K.E., Moldowan, J.M., 1991. Effects of source, thermal maturity and biodegradation on the distribution and isomerization of homohopanes in petroleum. Organic Geochemistry 17, 47–61.
Peters, K.E., Moldowan, J.M., 1993. The Biomarker Guide. Interpreting Molecular Fossils in Petroleum and Ancient Sediments. Prentice Hall, Englewood Cliffs, New Jersey.
Peters, K.E., Walters, C.C., Moldowan, J.M., 2005. The Biomarker Guide, second ed. Cambridge University Press, UK.
Reinhardt, J.W., Hoogendijk, F., Al-Riyami, R., Amthor, J.E., Williams, G., Frewin, N.L., 1998. Cambrian intra-salt carbonate stringers of South Oman: reviving a complex exploration play. GEO'98 Abstracts in GeoArabia 3, 145–146.
Robinson, N., Eglinton, G., 1990. Lipid chemistry of icelandic hot spring microbial mats. Organic Geochemistry 15, 291–298.
Schröder, S., Grotzinger, J.P., 2007. Evidence of anoxia at the Ediacaran–Cambrian boundary: the record of redox-sensitive trace elements and rare earth elements in Oman, vol. 164. Journal of the Geological Society, London. pp. 175–187.
Sinninghe Damsté, J.S., Kenig, F., Koopmans, M.P., Köster, J., Schouten, S., Hayes, J.M., de Leeuw, J.W., 1995. Evidence for gammacerane as an indicator of water column stratification. Geochimica et Cosmochimica Acta 59, 1895–1900.
Sofer, 1980. Preparation of carbon dioxide for stable carbon isotope analysis of petroleum fractions. Analytical Chemistry 52, 1389–1391.
Summons, R.E., Brassell, S.C., Eglinton, G., Evans, E., Horodyski, R.J., Robinson, N., Ward, D.M., 1988a. Distinctive hydrocarbon biomarkers from fossiliferous sediment of the late Proterozoic Walcott Member, Chuar Group, Grand Canyon, Arizona. Geochimica et Cosmochimica Acta 52, 2625–2637.
Summons, R.E., Jahnke, L.L., Logan, G.A., Hope, J.M., 1999. 2-Methylhopanoids as biomarkers for cyanobacterial oxygenic photosynthesis. Nature 398, 554–557.
Summons, R.E., Powell, T.G., 1992. Hydrocarbon composition of the Late Proterozoic oils of the Siberian Platform: implications for the depositional environment of the source rocks. In: Schidlowski, M., Golubic, S., Kimberley, M.M., McKirdy, D.M., Trudinger, P.A. (Eds.), Early Evolution and Mineral and Energy Resources. Proceedings of IGCP Project , vol. 157. Maria Laach, 1988. Springer Verlag, Berlin, pp. 296–307.
Summons, R.E., Powell, T.G., 1987. Identification of aryl isoprenoids in source rocks and crude oils: Biological markers for green sulphur bacteria. Geochimica et Cosmochimica Acta 51, 557–566.
Summons, R.E., Powell, T.G., Boreham, C.J., 1988b. Petroleum geology and geochemistry of the Middle Proterozoic McArthur Basin, Northern Australia. III. Composition of extractable hydrocarbons. Geochimica et Cosmochimica Acta 52, 1747–1763.
Terken, J.M.J., Frewin, N.L., 2000. The Dhahaban petroleum system of Oman. American Association of Petroleum Geologists Bulletin 84, 523–544.
Terken, J.M.J., Frewin, N.L., Indrelid, S.L., 2001. Petroleum systems of Oman: charge timing and risks. American Association of Petroleum Geologists Bulletin 85, 1817–1845.
Thiel, V., Jenisch, A., Wörheide, G., Löwenberg, A., Reitner, J., Michaelis, W., 1999. Mid-chain branched alkanoic acids from "living fossil" demosponges: a link to ancient sedimentary lipids? Organic Geochemistry 30, 1–14.
Van Graas, G., de Lange, F., de Leeuw, J.W., Schenck, P.A., 1982. A-nor-steranes, a novel class of sedimentary hydrocarbons. Nature 296, 59–61.
Volkman, J.K., 2003. Sterols in microorganisms. Applied Microbiology and Biotechnology 60, 495–506.
Williams, L.A., 1984. Subtidal stromatolites in Monterey Formation and other organic-rich rocks as suggested contributors to petroleum formation. American Association of Petroleum Geologists Bulletin 68, 1879–1893.